

Effects of Cardiac Troponin I Mutation P83S on Contractile Properties and the Modulation by PKA-Mediated Phosphorylation

Yuanhua Cheng,^{†,||} Steffen Lindert,[§] Lucas Oxenford,[†] An-yue Tu,[†] Andrew D. McCulloch,^{||,⊥} and Michael Regnier^{*,†,‡}

[†]Department of Bioengineering, University of Washington, Seattle, Washington 98105, United States

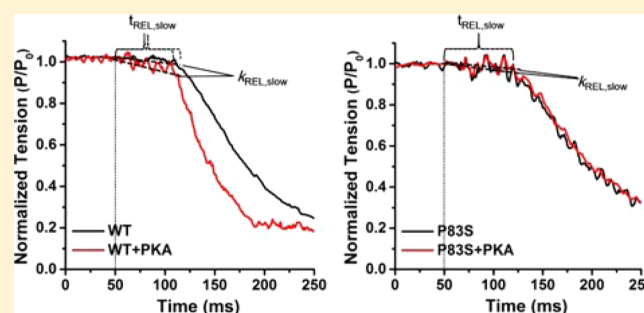
[‡]Center for Cardiovascular Biology, University of Washington, Seattle, Washington 98195, United States

[§]Department of Chemistry and Biochemistry, The Ohio State University, Columbus, Ohio 43210, United States

^{||}National Biomedical Computation Resource, University of California San Diego, La Jolla, California 92093, United States

[⊥]Department of Bioengineering, University of California San Diego, La Jolla, California 92093, United States

ABSTRACT: cTnI^{P82S} (cTnI^{P83S} in rodents) resides at the I-T arm of cardiac troponin I (cTnI) and was initially identified as a disease-causing mutation of hypertrophic cardiomyopathy (HCM). However, later studies suggested this may not be true. We recently reported that introduction of an HCM-associated mutation in either inhibitory-peptide (cTnI^{R146G}) or cardiac-specific N-terminus (cTnI^{R21C}) of cTnI blunts the PKA-mediated modulation on myofibril activation/relaxation kinetics by prohibiting formation of intrasubunit contacts between these regions. Here, we tested whether this also occurs for cTnI^{P83S}. cTnI^{P83S} increased both Ca²⁺ binding affinity to cTn (K_{Ca}) and affinity of cTnC for cTnI (K_{C-I}), and eliminated the reduction of K_{Ca} and K_{C-I} observed for phosphorylated-cTnI^{WT}. In isolated myofibrils, cTnI^{P83S} maintained maximal tension (T_{MAX}) and Ca²⁺ sensitivity of tension (pCa₅₀). For cTnI^{WT} myofibrils, PKA-mediated phosphorylation decreased pCa₅₀ and sped up the slow-phase relaxation (especially for those Ca²⁺ conditions that heart performs *in vivo*). Those effects were blunted for cTnI^{P83S} myofibrils. Molecular-dynamics simulations suggested cTnI^{P83S} moderately inhibited an intrasubunit interaction formation between inhibitory-peptide and N-terminus, but this “blunting” effect was weaker than that with cTnI^{R146G} or cTnI^{R21C}. In summary, cTnI^{P83S} has similar effects as other HCM-associated cTnI mutations on troponin and myofibril function even though it is in the I-T arm of cTnI.



INTRODUCTION

Hypertrophic cardiomyopathy (HCM), a familial myocardial condition often correlated with myofilament contractile protein mutations, has been identified as a major autosomal dominant disease accompanied by a morbidity of 1 per 500 individuals.^{1,2} To date, over 900 HCM-associated mutations have been identified in 24 genes,^{3,4} and a majority of these mutations reside in the thick filament proteins, such as cardiac myosin binding protein C (cMyBP-C), myosin, and titin.^{4,5} Despite this, several mutations have also been reported in one of the thin filament regulatory proteins, cardiac troponin I (cTnI), which is the actomyosin ATPase inhibitory subunit of the cardiac troponin (cTn) complex.⁵ cTn is the key regulator for muscle contraction, and it regulates the thin and thick filaments interaction in a Ca²⁺-dependent manner.⁶ In diastole, cardiac troponin C (cTnC) presents in its “closed” conformation, and cTnI strongly binds with actin (weak interaction with cTnC), thus inhibiting actin–myosin interaction.^{6,7} In systole, with the rise of intracellular Ca²⁺ in cardiomyocytes, Ca²⁺ binding to the cTnC site II induces an “open” conformation of the regulatory N-domain and increases its interaction with cTnI switch-

peptide.^{6,8} Consequently, this results in a decreased binding of cTnI inhibitory-peptide with actin and increased tropomyosin mobility that the myosin binding sites were exposed on actin, thus allowing myosin interaction with actin and the formation of “cross-bridges”.⁶

During β -adrenergic stimulation, cTnI is phosphorylated by protein kinase A (PKA) at sites Ser-23/Ser-24 (S23/S24), which reside at the cardiac-specific N-terminus of cTnI.⁹ We¹⁰ and others^{9,11–13} have demonstrated that this PKA-mediated phosphorylation weakens cTnC–cTnI (C–I) interaction, decreases the Ca²⁺ sensitivity (pCa₅₀) of cardiac muscle tension production, increases Ca²⁺ dissociation rate (k_{off}) from cTnC, elevates cross-bridge cycling kinetics, and accelerates cardiac muscle relaxation. Additionally, we demonstrated that PKA phosphorylation of isolated rat cardiac myofibrils with WT-cTn accelerates and shortens the initial, slow-phase of relaxation

Special Issue: J. Andrew McCammon Festschrift

Received: February 24, 2016

Revised: May 4, 2016

Published: May 6, 2016

(especially during submaximal activation that the heart operates *in vivo*) that is considered to reflect cross-bridge detachment rate and, perhaps, deactivation of thin filament.¹⁰

Since the first HCM-associated cTnI mutations were reported by Kimura et al. in 1997,¹⁴ there have been at least 29 mutations in cTnI putatively suggested to be contributory to HCM.^{5,15} Initial studies by Niimura et al. identified cTnI^{P82S} (cTnI^{P83S} in rodents) as a disease-causing mutation of the late-onset hypertrophy, and its pathogenicity is not clear.¹⁶ Later on, Frazier et al. reported an African American individual (32-year-old, women) with severe HCM (a family history of HCM and sudden cardiac death), and identified that she has both the P82S mutation in cTnI and the R453S mutation in cardiac β -myosin heavy chain (MYH7).¹⁷ By analyzing DNA from a panel of 100 individuals, Frazier et al. also determined that cTnI^{P82S} presents in $\sim 3\%$ of healthy African Americans. Thus, they concluded that cTnI^{P82S} is likely a non-disease-causing amino acid variant.¹⁷ Using transgenic mice, Ramirez-Correa et al. reported that cTnI^{P83S} showed normal cardiac contractility when young, but displayed diastolic dysfunction (for instance, impaired ejection and relaxation time, and prolonged isovolumetric relaxation time) with aging.¹⁸ Additionally, they found that cTnI^{P83S} mice blunted the β -adrenergic response and impaired myofilament cooperativity.¹⁸ Considering this, it is of importance to further investigate whether cTnI^{P82S} alters myofibril contraction/relaxation kinetics, and whether structural–function changes are similar to those of other HCM-associated cTnI mutations.

Among all HCM cTnI mutations, cTnI^{R146G} (located in the inhibitory-peptide) and cTnI^{R21C} (resided at the cardiac-specific N-terminus) have been extensively studied by several groups.^{19–33} Recently, we also reported the blunted β -adrenergic response for both cTnI HCM-associated mutations.^{34,35} Both mutations significantly left-shifted (increased) Ca^{2+} binding affinity to cTn (K_{Ca}) and the affinity of cTnC for cTnI ($K_{\text{C-I}}$). PKA-mediated phosphorylation of cTnI induced a similar reduction of K_{Ca} for all complexes, but the reduction in $K_{\text{C-I}}$ normally seen with cTnI^{WT} did not occur for either mutation in cTnI. Both mutations increased Ca^{2+} sensitivity of tension (pCa_{50}) while maximal tension (T_{MAX}) was maintained. PKA-mediated phosphorylation of cTnI right-shifted pCa_{50} for cTnI^{WT} myofibrils, however not for either mutation.³⁴ PKA-mediated phosphorylation also sped up the initial, slow-phase relaxation for cTnI^{WT} myofibrils, especially at those submaximal Ca^{2+} conditions that the heart performs *in vivo*. Importantly, this effect on relaxation was eliminated for both cTnI^{R146G} and cTnI^{R21C} myofibrils, as was PKA-mediated reduction in $K_{\text{C-I}}$.³⁴ Our results also suggested that the structural basis of how these two mutations blunted the ability of PKA-mediated phosphorylation on cTnC–cTnI interaction, myofibril contraction, and relaxation is prohibiting the formation of an intrasubunit contact between the cTnI N-terminus (NcTnI) and the inhibitory-peptide of cTnI, which further precipitates reduction of interaction between the cTnI switch-peptide and cTnC hydrophobic-patch.^{34,35}

To understand whether the above effects occur in all HCM-associated cTnI mutations or they are restricted to the mutations in specific regions (such as N-terminus, inhibitory-peptide region), in the present work, we studied the HCM-associated mutation cTnI^{P83S} that is located in the I-T arm region (see Figure 1 for the location). Compared to cTnI^{WT}, cTnI^{P83S} also increased K_{Ca} and $K_{\text{C-I}}$, similar to what we previously reported on cTnI^{R146G} and cTnI^{R21C}, but with less

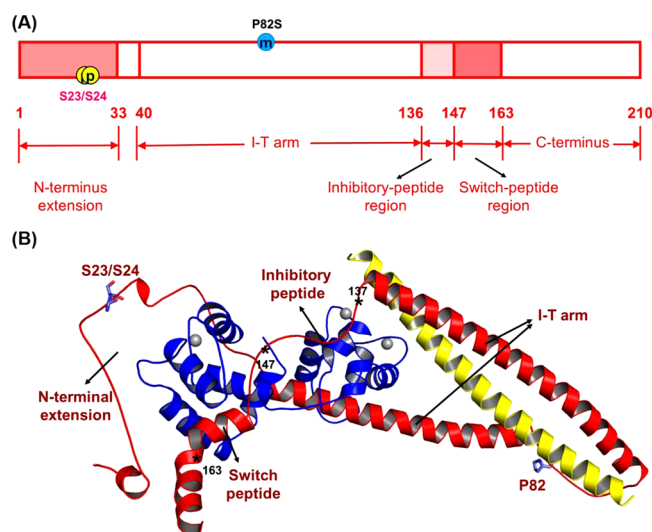


Figure 1. Human cTnI sequence (A) and ternary structure (B) with HCM-related mutation site (P82S) and PKA-mediated phosphorylation sites (Ser-23/Ser-24). Here, in the ternary structure, cTnC (1–161) is shown in blue; cTnI (1–172) is in red, and cTnT (236–285) is in yellow. The asterisks indicate the key positions in cTnI, in which residues 137–146 form the inhibitory-peptide of cTnI and residues 147–163 belong to the switch-peptide of cTnI.

degree (extent) of increment. Introduction of the bis-phosphomimic substitutions on cTnI^{P83S} eliminated the reduction of $K_{\text{C-I}}$ normally seen in cTnI^{WT}; however, it also blunted the reduction of K_{Ca} that is detected in both cTnI^{WT}, cTnI^{R146G} and cTnI^{R21C}. In isolated myofibrils, both pCa_{50} and T_{MAX} were maintained for cTnI^{P83S} exchanged myofibril, but with PKA-mediated phosphorylation, cTnI^{P83S} also eliminated the right-shift of pCa_{50} normally seen with cTnI^{WT} exchanged myofibrils. Our computational modeling results suggested that cTnI^{P83S} moderately inhibited the formation of the intrasubunit interaction between cTnI inhibitory-peptide and NcTnI that is normally observed for WT-cTn with phosphorylation of cTnI S23/S24; however, this “blunting” effect was much weaker than cTnI^{R146G} and cTnI^{R21C}. Thus, cTnI^{P83S} appears to have effects on cTn and myofibril function similar to HCM-associated mutations in the N-terminus and inhibitory-peptide regions of cTnI, but the effect on Ca^{2+} sensitivity of myofibril tension and PKA modulation of relaxation may be more moderate, and this may at least partially explain conflicting reports and conclusions in the literature.

EXPERIMENTAL AND THEORETICAL METHODS

Proteins, cTnC Labeling, cTnI Phosphorylation, and cTn Complex Reconstitution. WT rat cTnC, cTnI, and cTnT were constructed and expressed as described previously.³⁶ cTnC^{C35S}, cTnI^{S23D/S24D}, cTnI^{P83S}, and cTnI^{P83S/S23D/S24D} were constructed from WT cTnC and cTnI plasmids, respectively, using a site-directed mutagenesis kit (Stratagene, La Jolla, CA). All WT and mutant proteins were expressed with a pET-24 vector (Novagen, Madison, WI) which contains a T7 promoter, a lac operator, and a kanamycin resistant gene. Finally, the expressed constructs were confirmed by DNA sequence analysis.

The cTnC^{C35S} substitution was labeled with a fluorescent probe {N-[2-(iodoacetoxy)ethyl]-N-methylamino-7-nitrobenz-2-oxa-1,3-diazole (IANBD, $M_w = 406.14$, Life technologies, Cat No: I-9) at position C84 (cTnC^{C35S}_{IANBD}) in the dark overnight at

4 °C to monitor the Ca^{2+} –cTn (K_{Ca}) and cTnC–cTnI ($K_{\text{C-I}}$) binding affinities, as described previously.^{10,34,37–40} The labeling efficiency (also known as percentage of labeling) was obtained by comparing the IANBD fluorophore versus protein concentration ratio.^{10,39} The protein's concentration was determined using the Bio-Rad protein assay (based on the Bradford method), and the IANBD fluorophore concentration was computed using the maximal absorbance of labeled protein at a wavelength ~ 481 nm dividing by IANBD's extinction coefficient ($21\,000\text{ M}^{-1}\text{cm}^{-1}$).^{10,39} The labeling efficiency of cTnC^{C35S} substitution was $\sim 90\%$. Whole cTn complexes were formed using rat cTnC (WT or cTnC^{C35S}_{IANBD}), rat cTnI (WT, S23D/S24D, P83S, or P83S/S23D/S24D), and rat cTnT (WT) at a 1:1:1 molar ratio and then dialyzed through a series of buffers with gradually decreased KCl concentration at 4 °C (without stirring) as described previously.^{41,42} Here, cTn complexes with cTnC^{C35S}_{IANBD}, cTnI^{S23D/S24D} (or cTnI^{P83S/S23D/S24D}) were only used for Ca^{2+} –cTn (K_{Ca}) binding measurement.

Steady-State Fluorescence Measurements. Steady-state fluorescence measurements were performed by a luminescence spectrometer (PerkinElmer LS50B) at 15 °C as described previously.^{10,34,39,40} Solution applied for this measurement contains (in mM) the following: 150 KCl, 20 MOPS, 3 MgCl_2 , 2 EGTA, and 1 DTT (pH 7.0). Fluorescence signal was recorded at ~ 530 nm during the titration of (1) Ca^{2+} into 2 mL of cTnC^{C35S}_{IANBD} (0.6 μM), or (2) cTnI variants (WT, S23D/S24D, P83S or P83S/S23D/S24D) into 2 mL of cTnC^{C35S}_{IANBD} (0.6 μM) in the presence of Ca^{2+} (100 μM). The concentration of free Ca^{2+} was computed using Maxchelator.⁴³ The Ca^{2+} sensitivity (measured as pCa_{50} , the pCa ($\text{pCa} = -\log[\text{Ca}^{2+}]$) value at half-maximal fluorescence signal change) was collected by fitting the titration curve with the S-shaped Hill equation as described previously.⁴⁴ Here, the reported data are the means \pm SE of 4–6 successive titrations.

Ethical Approval and Tissue Preparation. All animal procedures were carried out according to the U.S National Institutes of Health Policy on Humane Care and Use of Laboratory Animals and were approved by the University of Washington (UW) Institutional Animal Care and Use Committee (IACUC). Animals were housed in the Department of Comparative Medicine at UW and cared for in accordance with UW IACUC procedures. After initial exposure to isoflurane (3–5% in oxygen), pentobarbital (50 mg/kg) was intraperitoneal injected to male, Sprague–Dawley rats (3 months old, 150–250 g) for anesthesia. When the rat had no reflexive response, its heart was quickly excised and dissected in oxygenated physiological saline solution, which contains (in mM) the following: 100 NaCl, 2.5 KCl, 24 NaHCO_3 , 1 Na_2HPO_4 , 1 $\text{MgSO}_4 \cdot 7\text{H}_2\text{O}$, and 1 CaCl_2 .⁴⁵ After this, both ventricles were cut open, and the whole heart was demembranated in skinning solution containing (in mM) the following: 100 KCl, 9 MgCl_2 , 4 Na_2ATP , 5 K_2EGTA , 10 MOPS, 1% Triton X-100, pH 7.0, 50% v/v glycerol, and 1:100 dilution Protease-Inhibitor-Cocktail (PI) (Sigma-Aldrich, Cat. No.: P8340) overnight at 4 °C.^{46,47} The heart was then washed three times in the same buffer without Triton X-100 and kept at -20 °C for use for up to 1 week. Myofibrils from the left ventricles (LV) were used for the mechanical measurements described below.

Solutions. Solution composition (for mechanical measurements) was determined using an iterative algorithm, which calculates the equilibrium concentration of ligands and ions

according to published affinity constants.⁴⁸ The relaxing solution has the composition as follows (in mM): 80 MOPS, 1 Mg^{2+} , 5 MgATP , 15 EGTA, 52 Na^+ , 83 K^+ , and 15 creatine phosphate (CP), pH 7.0 at 15 °C. The inorganic P_i concentration was 0.5 mM (determined by NMR), and the solution ionic strength was 170 mM.⁴⁹ All mechanical measurements were carried out at 15 °C. The Ca^{2+} levels (measured as pCa) of activating solutions were adjusted by adding CaCl_2 .

Exchange of Recombinant cTn Complexes into Myofibrils. Muscle bundles obtained from the rat LV were rinsed twice in Rigor solution, with a composition of (in mM) the following: 100 KCl, 50 Tris, 1 EGTA, 2 MgCl_2 , 1 DTT, and 1:100 dilution of PI. Then, the muscle bundles were homogenized for two 30 s pulses at a high speed on ice. cTn complexes containing cTnI^{WT} or cTnI^{P83S} (~ 1 mg/mL) were passively exchanged into isolated rat myofibrils in a buffer containing (in mM) the following: 150 KCl, 5 MgCl_2 , 20 MOPS, 4 ATP, 2 EGTA, 1 DTT, and 1:100 dilution of PI (pH 7.0) on a slow rocker overnight at 4 °C.^{10,34} Following overnight exchange, myofibrils were washed with relaxing buffer containing ~ 1 mg/mL bovine serum albumin (BSA) twice for 30 min to remove any nonspecifically bound exogenous cTn. Myofibrils were then equally split: one-half was used to collect the kinetic/mechanism results prior to PKA treatment, and the other half was incubated with 200 μL relaxing solution containing 100 units of PKA and 6 mM DTT for 45 min at 20 °C for studying the effects of PKA-mediated phosphorylation.

Myofibril Mechanical and Kinetics Measurements. Myofibril mechanical/kinetics studies were carried out on a home-built setup as described previously.^{10,50,51} In brief, single or small bundles of ~ 2 –4 cardiac myofibrils were attached between two glass microneedles (one is straight and another is bent) forged from borosilicate glass capillary tubes (OD 1.0 mm, ID 0.5 mm, Sutter Instruments, Novato, CA), and perfused with activating and relaxing buffers that can be rapidly switched. The initial sarcomere length (SL) of myofibril was set as ~ 2.3 μm . Here, the straight microneedle is mounted to one end of the myofibril and was applied to rapidly shorten and restretch the myofibril through a computer interface and a piezocontroller motor (PZT Servo controller, LVPZT amplifier, Physik Instrumente, Irvine CA). The bent microneedle acts as a force transducer (FT) to hold the other end of the myofibril, and it deflected with application of force in a predictable mode.⁵⁰ The stiffness of FT applied for this study ranged from 5 to 9 $\text{nN } \mu\text{m}^{-1}$, and the value was measured under a 40 \times lens by bending the microneedle with a set of force using a galvanometer. The displacement of FT was recorded by a dual-diode system, and correlated to tension development. At the end of each experiment, a calibration curve was performed in which the FT needle was moved in 1 μm steps using micromanipulators (MP-285, Sutter Instruments, Novato, CA) over the range of the diodes. The relaxing (10^{-9} M, pCa 9.0) and activating (10^{-4} M, pCa 4.0) Ca^{2+} solutions were streamed by a homemade double-barreled borosilicate theta glass pipet (capillary glass tubing OD 2.0 mm, ID 1.4 mm, SEP 0.2 mm, modified in house to OD of 0.65 mm, Warner Instruments, Hamden, CT) to the attached myofibrils. The solutions were stepping an increase or decrease over the mounted preparation, and this rapid switch (within ~ 10 ms) was controlled by a computerized motor (SF-77B Perfusion

Fast Step, Warner Instruments Corporation, Hamden, CT).^{50–52}

Activation–relaxation results were measured at 15 °C and then fit as described previously.^{50,52–54} The kinetics of myofibril activation (k_{ACT}) with a rapid increase in Ca^{2+} level was collected from a single exponential rise to a maximum. Once the myofibril was activated, a rapid release–restretch protocol (the myofibril was 20% shorting in optimal length suddenly, and after 25 ms of unloaded shortening period, the myofibril was rapidly stretching back to the original length) was applied to get the rate of tension redevelopment (k_{TR}).⁵⁴ The rate of slow-phase relaxation ($k_{\text{REL,slow}}$) was computed from the slope of a regression line fit to the force trace and then normalized to the entire tension amplitude. The duration of slow-phase relaxation ($t_{\text{REL,slow}}$) was collected from the onset of buffer switching to the shoulder marking the starting of fast-phase relaxation. An apparent change in slope or in “signal-to-noise” ratio was applied to determine at the transition from slow- to fast-phase. The rate for fast-phase relaxation ($k_{\text{REL,fast}}$) was fitted by a single exponential decay. In some cases (decay cannot be well-described by a single exponential), a $t_{1/2}$ estimation was made and then converted to a rate $\tau = \ln(2)/t_{1/2}$. In this study, myofibrils that contracted over 10% of their optimal length were considered as nonisometric and excluded from the analysis.

cTnI Phosphorylation Profile. The cTnI phosphorylation profile was quantified using Western blot by calculating the amount of phosphorylated cTnI relative to the total amount of cTnI.^{10,34} The phosphorylated cTnI was detected using a rabbit polyclonal to cTnI (phospho S22 + S23, from abcam, cat. no.: ab58545) as primary antibody (1:1000) and goat antirabbit IgG-HRP (Santa Cruz Biotechnology, sc-2004) as secondary antibody (1:5000). The total cTnI was quantified using antibodies rabbit polyclonal IgG to troponin I (H170, from Santa Cruz Biotechnology, sc-15368) (1:1000) and goat antirabbit IgG-HRP (1:5000).

Computational Modeling. The initial structure of the cTn complex was built up on the basis of the crystal structure of Takeda et al.⁵⁵ with the addition of the N-terminus of cTnI from the NMR structure provided by Howarth et al.⁵⁶ To mimic phosphorylation, a bis-phosphomimics model (cTnI^{S23D/S24D}) was constructed by mutating S23/S24 of cTnI to aspartic acid (D). Two systems of human cTn were prepared for simulations: a cTnI^{P83S} Ca^{2+} -bound cTnC_{1–161}-cTnI_{1–172}-cTnT_{236–285} (cTnI^{P83S} cTn model), and a cTnI^{P83S/S23D/S24D} Ca^{2+} -bound cTnC_{1–161}-cTnI_{1–172}-cTnT_{236–285} (cTnI^{P83S/S23D/S24D} cTn model). The cTnI mutations were introduced by using the Mutate Residue Module in VMD.⁵⁷ The models were immersed in a truncated rectangular box with TIP3P water molecules, which extended minimally 14 Å away from any solute atoms.⁵⁸ Then, K^+ and Cl^- ions were added to neutralize the systems, and brought to 150 mM ionic strength. The fully solvated systems contained 112 739 (cTnI^{P83S} cTn model) and 112 740 (cTnI^{P83S/S23D/S24D} cTn model) atoms, respectively. Prior to the MD simulations, we performed three steps of minimizations. Next, for each of the two simulation systems, three independent sets of 150 ns MD simulations were carried out under 300 K and the NPT ensemble using NAMD 2.9⁵⁹ and the CHARMM27 force field.⁶⁰ The SHAKE procedure was applied, and the time step was set as 2.0 fs.⁶¹ During the sampling process, the coordinates were saved every 10 ps (cTnI^{P83S} cTn model) and 2 ps (cTnI^{P83S/S23D/S24D} cTn model), respectively. The stability

between site II Ca^{2+} and its coordinating residues (Asp-65, Asp-67, Ser-69, Thr-71, Asp-73, and Glu-76) of cTnC was monitored by calculating the corresponding distances for each 150 ns simulation as described previously.^{34,35,39,62}

The residue–residue contacts between cTnC and key regions of cTnI (N-terminus, inhibitory-peptide, and switch-peptide regions) were monitored over the course of the entire 450 ns simulations. Contacts between two residues were defined as described previously, with a carbon–carbon distance of ≤ 5.4 Å and a distance between any other noncarbon atoms of ≤ 4.6 Å being a contact.^{39,62} Contacts between the NcTnC-switch-peptide of cTnI and cTnC-inhibitory-peptide of cTnI were monitored. The intrasubunit contact between N-terminus and inhibitory-peptide of cTnI were also recorded. For each contact pair, the portion of the simulation time that these residues contacted with each other was calculated for both simulation systems. Lastly, an I–T arm interhelical angle analysis was performed. The interhelical angles were computed using interhix (K. Yap, University of Toronto). We calculated the angle between the two structural helices in cTnI as defined by cTnI residues 45–82 and 91–137.

Statistics. Comparison between groups of data was carried out using the one-way analysis of variant (ANOVA) test as appropriate. All experimental data are expressed as mean \pm SE, and n represents the number of experimental samples in each group; the reported computational (MD simulations) results are expressed as mean \pm SD, and n equals 3. Results with $p < 0.05$ were considered statistically significant.

RESULTS

Steady-State Fluorescence Measurements of K_{Ca} and $K_{\text{C-I}}$. The effects of cTnI^{P83S} mutation \pm bis-phosphomimic substitutions on cTn- K_{Ca} and $K_{\text{C-I}}$ were determined by steady-state fluorescence measurements using a fluorophore IANBD, as previously described.^{10,34,39} IANBD, a sulfhydryl-reactive and environment-sensitive extrinsic fluorophore, has been widely applied for monitoring the intramolecular interactions of proteins. The labeling of IANBD at C84 of cTnC^{C35S} reflects conformational and environmental changes of NcTnC that arise from Ca^{2+} binding and/or interaction with cTnI.^{10,34,38,39} We first measured the conformational changes with Ca^{2+} binding to cTn containing either cTnI^{P83S} or cTnI^{P83S/S23D/S24D} compared with the cTnI^{WT} set. As shown in the Ca^{2+} titration curves (Figure 2A), the Ca^{2+} sensitivity of the fluorescence intensity (reported as pCa_{50}) was left-shifted 0.09 pCa units, from 7.18 ± 0.02 (cTn with cTnI^{WT}) to 7.27 ± 0.02 (cTn with cTnI^{P83S}). Consistent with our previous finding,^{10,34} introduction of bis-phosphomimic substitutions on cTnI^{WT} (cTnI^{S23D/S24D}) also reduced K_{Ca} , resulting in a 0.27 pCa unit decrease (right-shifted to 6.91 ± 0.03). Interestingly, with introduction of bis-phosphomimic substitutions on cTnI^{P83S}, this effect was completely eliminated ($\text{pCa}_{50} = 7.24 \pm 0.03$ for cTn with cTnI^{P83S/S23D/S24D}).

cTnC-cTnI (C–I) interaction acts as a “gatekeeper” in transferring Ca^{2+} signal to other myofilament proteins to initiate cardiac muscle contraction. Therefore, we next measured how introduction of cTnI^{P83S} mutation \pm bis-phosphomimic substitutions affects the affinity of cTnC for cTnI ($K_{\text{C-I}}$). As shown in Figure 2B, the IANBD fluorescence signal increased with the titration of cTnI in solution containing $0.6 \mu\text{M}$ cTnC^{C35S}_{IANBD}, and there was no further increase beyond $0.6 \mu\text{M}$ cTnI, suggesting strong binding of cTnI to cTnC such that 1:1 binding was achieved. Similar to K_{Ca} , cTnI^{P83S} also left-

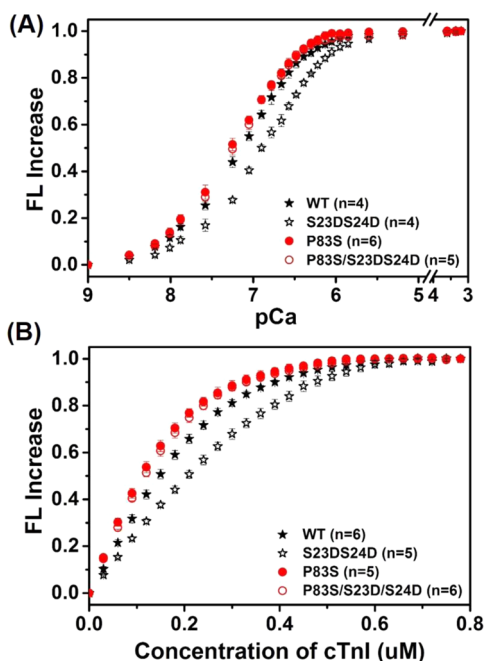


Figure 2. IANBD fluorescence emission intensity changes of (A) cTnC^{C35S} in complex with cTnI^{WT} and cTnI variants with titration of Ca²⁺ and (B) of cTnC^{C35S} alone with titration of cTnI variants.

shifted K_{C-I} compared to cTnI^{WT}. As we reported previously,^{10,34} bis-phosphomimic substitutions of cTnI^{WT} (cTnI^{S23D/S24D}) also reduced K_{C-I} . However, this effect was completely blunted for the cTnI^{P83S} mutant.

Recombinant Troponin (cTn) Complex Exchange Profiles. The native cTn in isolated myofibrils was passively exchanged with recombinant rat cTn containing either cTnI^{WT} or cTnI^{P83S}. The extent of exchange (exchange efficiency) for this procedure was periodically determined by exchanging cTn containing a cTnT labeled at the N-terminus with a c-myc tag, to compare the c-myc tag band versus the native cTnT band in gels and with Western blot analysis.¹⁰ We consistently saw >80% endogenous cTn replacement by cTn containing the c-myc tagged cTnT in myofibrils using this approach,¹⁰ suggesting our exchange protocol is very efficient and changes in contractile parameters should be attributed to the exchanged cTn containing cTnI^{P83S}.

In this study, we did five batches of passive exchange for both cTn species containing either cTnI^{WT} or cTnI^{P83S} at the same time. Following exchange and washing, myofibrils were equally split into two parts, with one-half used to collect the kinetics/mechanics results before PKA phosphorylation, and the other half to study the effects of PKA-mediated phosphorylation (see [Methods](#) section). The phosphorylation profile for cMyBP-C and titin (which can also be phosphorylated by PKA incubation) was not measured; however, this should be quite similar for each group as paired comparisons of myofibrils containing cTnI^{P83S} versus cTnI^{WT} were made from each heart. Rats generally have high β -adrenergic stimulation; thus, the native myofibrils (directly from the rats) displayed higher PKA phosphorylation levels of cTnI. Since the recombinant cTn containing either cTnI^{WT} or cTnI^{P83S} was not phosphorylated, the cTnI phosphorylation extent in exchanged myofibrils (prior to PKA treatment) was inversely correlated with the exchange efficiency. As shown in [Figure 3A](#), a fairly small amount of residual phosphorylated cTnI was present in every exchange

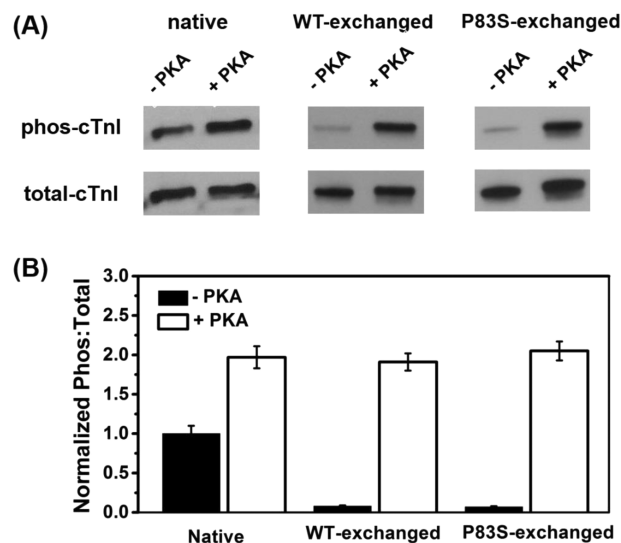


Figure 3. Raw (A) and normalized (B) PKA phosphorylation profile of cTnI for myofibrils exchanged with cTnI^{WT} or cTnI^{P83S} before and after PKA treatment.

preparation since the exchange efficiency was not 100%. In a comparison of the cTnI phosphorylation extent for native versus exchanged myofibrils (prior to PKA treatment), the exchange efficiencies for cTn containing cTnI^{WT} and cTnI^{P83S} were 89% and 91%, respectively, further confirming high exchange efficiency. After PKA treatment, the cTnI phosphorylation level was significantly increased, resulting in a high level of cTnI phosphorylated, which is consistent with our previous observation.^{10,34}

cTnI-P83S Mutation Has No Effects on Myofibril Contraction and Relaxation. The effect of cTnI^{P83S} mutation on tension development and relaxation kinetics (at 15 °C) was determined from isolated rat LV cardiac myofibrils exchanged with cTn containing cTnI^{P83S}, and then compared with the WT cTn complex. Myofibrils mounted by two glass microtools were exposed to continually flowing pCa buffer that was rapidly switched, from relaxing buffer (pCa 9.0) to either maximal (pCa 4.0) or submaximal (pCa 5.4, pCa 5.6 and pCa 5.8) [Ca²⁺] buffer, and finally back to 9.0. Representative example tension traces for cTnI^{WT} and cTnI^{P83S} exchanged myofibrils during the submaximal [Ca²⁺] activation–relaxation protocol (at pCa 5.4) are presented in [Figure 4](#). The magnitude of tension and kinetic for rat LV myofibrils exchanged with cTn containing cTnI^{WT} or cTnI^{P83S} is summarized in [Table 1](#) and [Figures 5](#) and [6](#).

Maximal tension (T_{MAX}) did not differ for myofibrils exchanged with cTnI^{P83S} (74.5 ± 5.0 mN/mm²) compared with cTnI^{WT} myofibrils (74.6 ± 5.8 mN/mm², [Figure 5A](#)). Tension was also measured at multiple submaximal Ca²⁺ levels, and the pCa₅₀ was just slightly left-shifted ($p > 0.05$, not statistic significantly, [Figure 5B](#)), from 5.32 ± 0.03 (cTnI^{WT} myofibrils) to 5.36 ± 0.03 (cTnI^{P83S} myofibrils), demonstrating that cTnI^{P83S} mutation did not have effects on the Ca²⁺ sensitivity of tension. This finding is clearly demonstrated in the example tension traces that were collected at pCa 5.4 ([Figure 4](#)), showing that cTnI^{P83S} myofibrils have same/similar tension development compared to the cTnI^{WT} myofibrils.

The contractile activation rate (k_{ACT}) after rapid-switching of [Ca²⁺] solution from pCa 9.0 to 4.0 (or submaximal Ca²⁺ level) contains the kinetic of Ca²⁺-mediated thin filament activation,

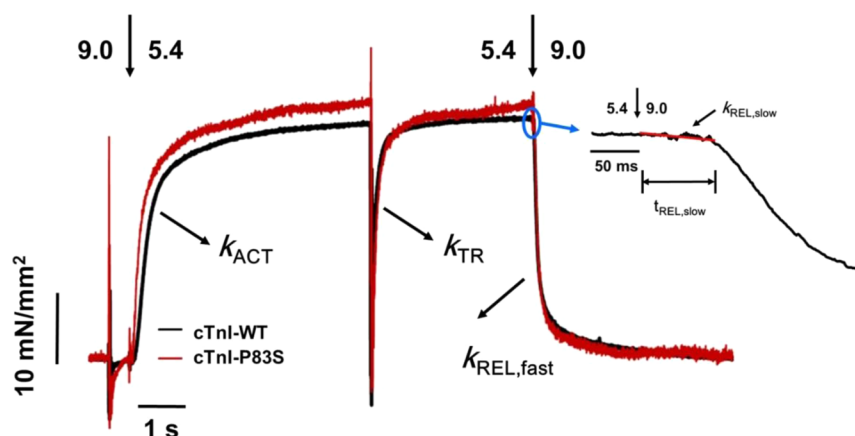


Figure 4. Representative tension trace (at pCa 5.4) for isolated rat cardiac myofibril after exchanging with recombinant cTn complexes containing cTnI^{WT} and cTnI^{P83S}. The inset is a close up of slow-phase of relaxation demonstrating how $k_{REL,slow}$ and $t_{REL,slow}$ are measured.

Table 1. Tension Generation and Relaxation Parameters after Recombinant Rat cTn Containing Either cTnI-WT or cTnI-P83S Exchange into Rat Ventricular Myofibrils at 15°C^a

myofibril batches	tension generation		k_{TR} (s ⁻¹)	relaxation		
	tension (mN/mm ²)	k_{ACT} (s ⁻¹)		slow-phase		fast phase $k_{REL,fast}$ (s ⁻¹)
				$t_{REL,slow}$ (ms)	$k_{REL,slow}$ (s ⁻¹)	
pCa = 4.0						
WT	74.6 ± 5.8 (16)	3.3 ± 0.3 (16)	5.3 ± 0.5 (16)	72 ± 3 (16)	0.9 ± 0.1 (16)	17 ± 2 (16)
WT+PKA	71.1 ± 6.5 (17)	2.5 ± 0.2* (17)	5.2 ± 0.7 (17)	63 ± 3* (16)	1.6 ± 0.2* (16)	17 ± 2 (16)
P83S	74.5 ± 5.0 (22)	3.7 ± 0.2* ^s (22)	6.1 ± 0.5 (22)	71 ± 2 (22)	1.0 ± 0.1* ^s (22)	18 ± 2 (22)
P83S+PKA	70.3 ± 3.9 (23)	3.5 ± 0.3* ^s (23)	5.9 ± 0.4 (22)	74 ± 3* ^s (22)	1.1 ± 0.2* ^s (22)	19 ± 2 (22)
pCa = 5.4						
WT	32.7 ± 3.6 (15)	1.8 ± 0.2 (15)	3.5 ± 0.4 (15)	67 ± 4 (15)	1.6 ± 0.2 (14)	17 ± 2 (15)
WT+PKA	21.5 ± 2.7* (16)	1.5 ± 0.2 (16)	3.1 ± 0.3 (15)	56 ± 4* (14)	3.7 ± 0.6* (14)	18 ± 3 (15)
P83S	35.7 ± 2.9* ^s (16)	2.1 ± 0.2 (16)	4.0 ± 0.3 (16)	67 ± 3* ^s (15)	1.9 ± 0.3* ^s (15)	17 ± 2 (16)
P83S+PKA	33.9 ± 2.4* ^s (15)	2.1 ± 0.2 (15)	3.8 ± 0.3 (14)	68 ± 4 (14)	2.2 ± 0.3 (14)	18 ± 1 (14)

^aValues given are mean ± SE. Number in parentheses is number of myofibrils. * $p < 0.05$ vs WT, and *^s $p < 0.05$ vs WT+PKA.

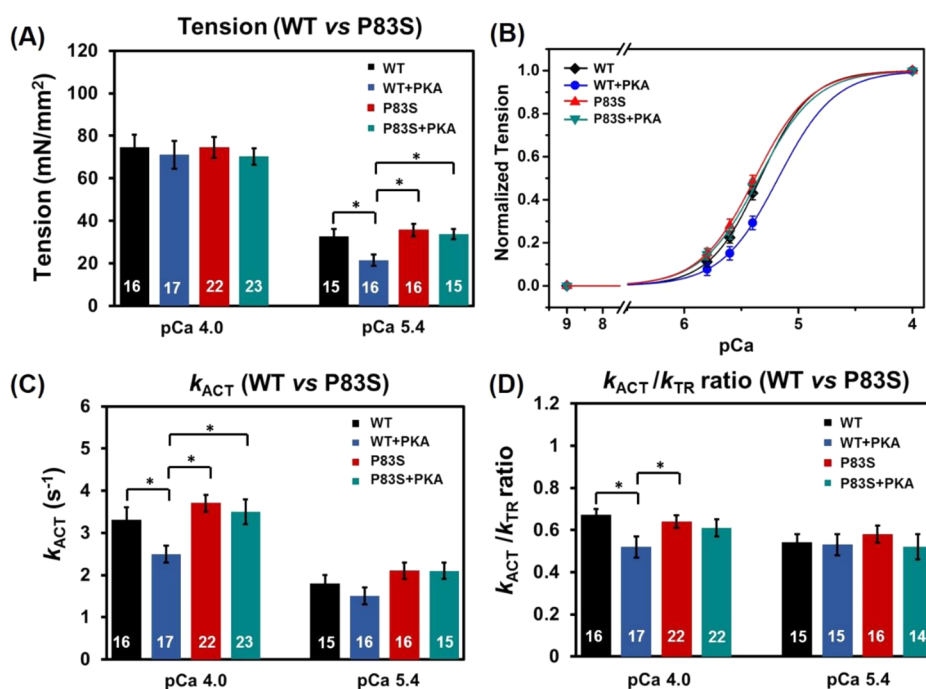


Figure 5. Tension (A), pCa-tension relationship (B), the kinetics of activation (C; k_{ACT}), and the k_{ACT}/k_{TR} ratio (D) for cTnI^{WT} vs cTnI^{P83S} exchanged myofibrils prior to and after PKA treatment. * $p < 0.05$.

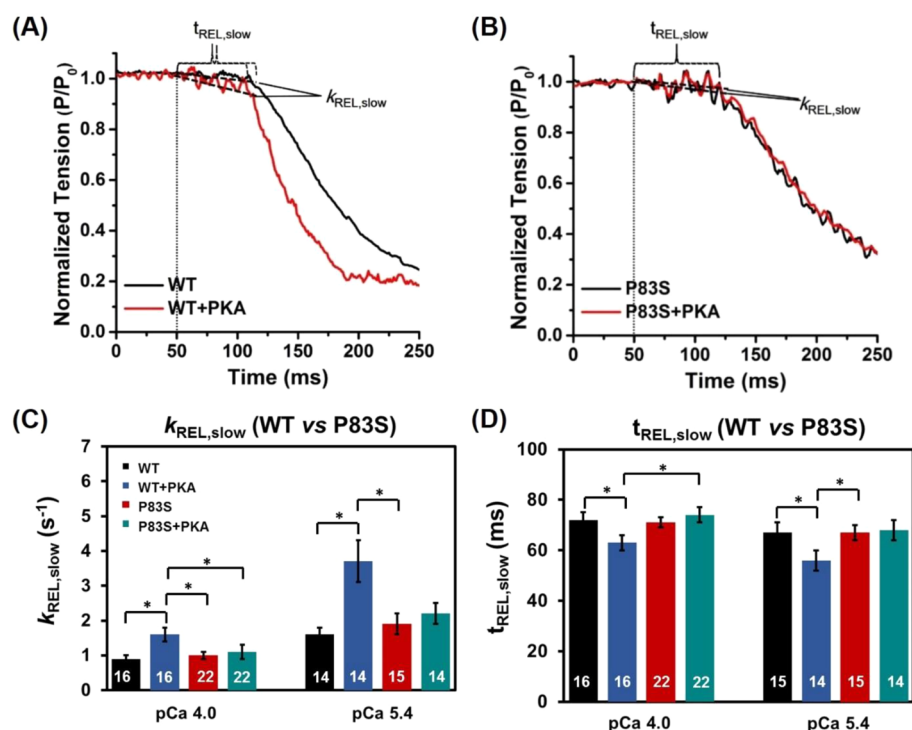


Figure 6. Slow-phase relaxation at submaximal Ca^{2+} level for (A) WT-cTn and (B) cTnI^{P83S} cTn exchanged rat cardiac myofibrils before (black) and after (red) PKA treatment. The kinetics (C; $k_{REL,slow}$) and duration (D; $t_{REL,slow}$) of slow-phase relaxation for cTnI^{WT} vs cTnI^{P83S} exchanged myofibrils prior to and after PKA treatment. * $p < 0.05$.

the subsequent myosin cross-bridge binding, as well as tension development. With respect to the cTnI^{WT} exchanged myofibrils ($3.3 \pm 0.3 \text{ s}^{-1}$), k_{ACT} did not differ for the cTnI^{P83S} ($3.7 \pm 0.2 \text{ s}^{-1}$) exchanged myofibrils either pCa 4.0, or pCa 5.4 (Figure 5C). As previously reported for rodent (or canine) cardiac myofibrils,^{10,34,49,54} k_{ACT} was significantly slower at submaximal Ca^{2+} activation than during maximal Ca^{2+} levels for both cTnI^{WT} and cTnI^{P83S} exchanged myofibrils, suggesting the Ca^{2+} sensitivity of cardiac contraction kinetics is also maintained upon introduction of the cTnI^{P83S} mutations. Once the activation was in or near steady-state, we applied a rapid release–restretch protocol on myofibrils to collect the rate of tension redevelopment (k_{TR}). This k_{TR} protocol is designed to measure the myosin cross-bridge attachment rate and the subsequent tension generation when Ca^{2+} –Tn binding is near steady-state (for example: thin filament is activated),⁴⁷ and thus can help to differentiate the contribution of Ca^{2+} -dependent thin filament activation vs cross-bridge cycling to k_{ACT} . For all measured conditions, k_{TR} was faster than k_{ACT} , as we previously reported,^{10,34} again suggesting thin filament activation (for rat cardiac myofibrils) is rate-limiting at 15 °C. Additionally, comparison of the k_{ACT}/k_{TR} ratio serves as a good indicator to show whether thin filament activation is more rate-limiting in the cTnI^{P83S} exchanged myofibrils with respect to the cTnI^{WT} exchanged myofibrils. Figure 4D demonstrates that the k_{ACT}/k_{TR} ratio did not change upon introduction of cTnI^{P83S} mutation.

The myofibrils were rapidly deactivated by a second switching from activating [Ca^{2+}] solution to relaxing solution (pCa 9.0), which induced a biphasic relaxation: an initial linear and slow decay followed by a rapid (fast) exponential tension decay back to the baseline (see the example tension trace in the inset of Figure 4). The slow-phase relaxation rate ($k_{REL,slow}$) predominantly reflects the cross-bridge detachment

rate,^{49,53,63–66} and the duration of slow-phase relaxation ($t_{REL,slow}$) represents the time for the troponin to move back to a “blocked” state.⁶⁷ For maximal activations, both $k_{REL,slow}$ ($0.9 \pm 0.1 \text{ s}^{-1}$ vs $1.0 \pm 0.1 \text{ s}^{-1}$, Figure 6C) and $t_{REL,slow}$ ($72 \pm 3 \text{ ms}$ vs $71 \pm 2 \text{ ms}$, Figure 6D) were unchanged for cTnI^{P83S} exchanged myofibrils compared to cTnI^{WT} exchanged myofibrils. In contrast to slow-phase, the much larger, fast-phase of relaxation ($k_{REL,fast}$) is influenced by multiple sarcomeric properties as well as uneven relaxation between sarcomeres in series.^{67,68} There was no difference in $k_{REL,fast}$ for cTnI^{P83S} ($18 \pm 2 \text{ s}^{-1}$) versus cTnI^{WT} myofibril ($17 \pm 2 \text{ s}^{-1}$) exchange. Similar to pCa 4.0, at submaximal Ca^{2+} level, there was also no difference in $k_{REL,slow}$, $t_{REL,slow}$, and $k_{REL,fast}$ between cTnI^{WT} and cTnI^{P83S} exchanged myofibrils. As we observed previously,^{64–66} $k_{REL,slow}$ was twice as fast at pCa 5.4 compared to the maximal activation (pCa 4.0) for all myofibrils (Table 1).

cTnI-P83S Mutation Blunts the PKA Effects on Myofibril Contraction and Relaxation. We next studied the effects of PKA-mediated phosphorylation on myofibril contraction and relaxation. Consistent with previous studies,^{10,34} with PKA treatment, T_{MAX} ($71.1 \pm 6.5 \text{ mN/mm}^2$, Figure 5A) was maintained for the cTnI^{WT} exchanged myofibrils, and pCa_{50} was right-shifted 0.18 pCa units to 5.14 ± 0.03 (Figure 5B), demonstrating the reduced Ca^{2+} sensitivity of tension development. At maximal Ca^{2+} level (pCa 4.0), PKA phosphorylation of cTnI^{WT} exchanged myofibrils also decreased k_{ACT} , whereas k_{TR} was maintained, suggesting that PKA phosphorylation affects the thin filament activation prior to cross-bridge binding and tension development. The above result can be clearly observed in the plots of the k_{ACT}/k_{TR} ratio from Figure 5D, demonstrating that this ratio is significantly decreased for PKA treated cTnI^{WT} exchanged myofibril compared with the ones prior to PKA treatment. After treating the cTnI^{P83S} exchanged myofibrils with PKA, T_{MAX} (70.3 ± 3.9

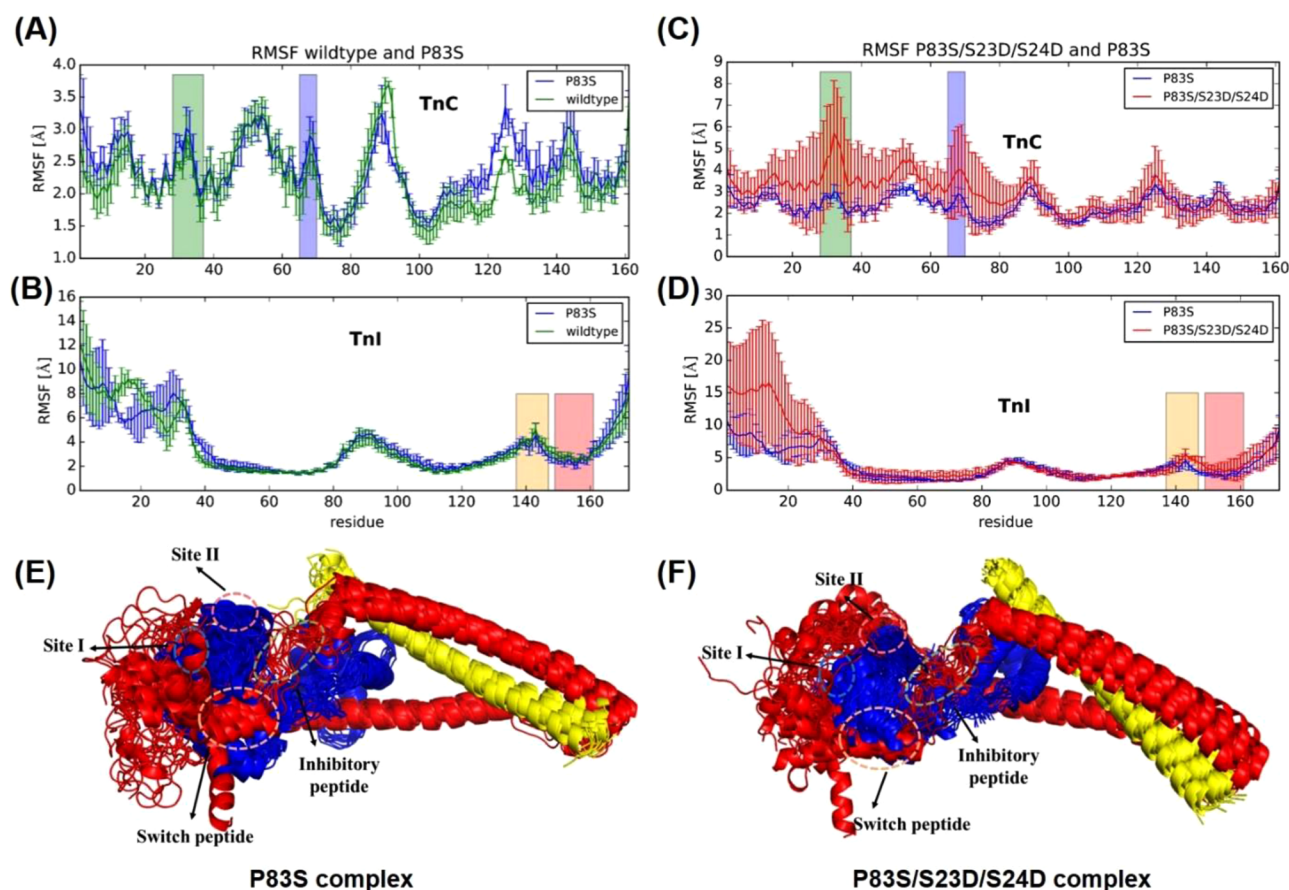


Figure 7. (A–D) Comparison of average (\pm SD) RMSF values of cTnC and cTnI for WT and cTnI^{P83S} and cTnI^{P83S/S23D/S24D} cTn systems in triplicate rounds of MD simulations. Here, site I and site II (the Ca²⁺ binding loop) of cTnC are highlighted in green and blue, respectively, and the inhibitory-peptide and switch-peptide regions of cTnI are highlighted in orange and pink, respectively. (E, F) The superposition of snapshots in cartoon representation extracted every 10 ns during 150 ns MD simulations for both complexes. The cTnC is shown in blue, cTnI is in red, cTnT is in gold, and all the key regions are highlighted with dashed circles.

mN/mm², Figure 5A) was also maintained; however, the Ca²⁺ sensitivity of tension development (pCa₅₀, Figure 5B) was not reduced (blunted) for cTnI^{P83S}. Additionally, maximal k_{ACT} did not change for cTnI^{P83S} exchanged myofibrils following PKA phosphorylation, which can be clearly seen by calculating the $k_{\text{ACT}}/k_{\text{TR}}$ ratio (Figure 5D), suggesting the slowed thin filament activation at maximal Ca²⁺ condition was also blunted.

A major influence of β -adrenergic stimulation on cardiac function is increasing heart rate, such that the rate of chamber relaxation needs to increase to allow for preserved diastolic filling. Thus, we studied how myofibril relaxation was influenced following PKA treatment of cTnI^{WT} and cTnI^{P83S} exchanged myofibrils. As we observed previously,^{10,34} PKA phosphorylation on cTnI^{WT} exchanged myofibrils significantly increased $k_{\text{REL,slow}}$ ($1.6 \pm 0.2 \text{ s}^{-1}$, Figure 6C) and reduced $t_{\text{REL,slow}}$ ($63 \pm 3 \text{ ms}$, Figure 6D) during maximal Ca²⁺ activation, thus speeding up the overall relaxation. Furthermore, the above effect was greater at submaximal Ca²⁺ level (pCa 5.4) where the heart operates. However, after treating the cTnI^{P83S} exchanged myofibrils with PKA, there was no change in either the rate ($1.1 \pm 0.2 \text{ s}^{-1}$, Figure 6C) or the duration ($74 \pm 3 \text{ ms}$, Figure 6D) of the slow-phase relaxation, suggesting that the effect of PKA phosphorylation on accelerating relaxation was blunted for cTnI^{P83S} mutation. The above finding can be clearly observed in Figure 6A,B, which is a set of example tension traces of slow-phase relaxation at submaximal Ca²⁺ level.

Molecular-Dynamics Simulations. Triplicate 150 ns MD simulations (three independent 150 ns simulations) were performed on both systems, the cTnI^{P83S} cTn system and the cTnI^{P83S/S23D/S24D} cTn system. Our first goal was to assess the effect of introduction cTnI^{P83S} mutation on the dynamics of cTn complex. To compare the dynamics of cTnI^{WT} versus cTnI^{P83S} cTn, triplicate MD simulations were performed and average RMSF (\pm SD) values for all residues were calculated. Figure 7A,B shows the average (\pm SD) RMSF of the cTnC and cTnI subunits for both cTnI^{WT} and cTnI^{P83S} cTn systems. As we previously saw for cTnI^{R21C} and cTnI^{R146G} mutations,³⁴ the fluctuations in the cTnI^{P83S} mutant were comparable to those in the WT system throughout most of the protein structure. The only pronounced difference was seen in the C-terminal domain of cTnC (cTnC residues 115–130), the loop connecting the two C-terminal cTnC EF-hand motifs (that interacts with the cTnI I–T arm). This is one direct consequence of cTnI^{P83S}, which located in the I–T arm region. Most other regions did not exhibit changes larger than the standard deviations. The largest fluctuations were observed in the NcTnI region, underscoring its highly flexible nature. With fluctuations this large, it is appropriate to refer to a range of conformations for NcTnI rather than an actual single structural conformation. The helical bundle known as the I–T arm (cTnI residues 45–82 and 91–137) comprised the most stable residues in the cTnI subunits, reflecting their structural rather than regulatory

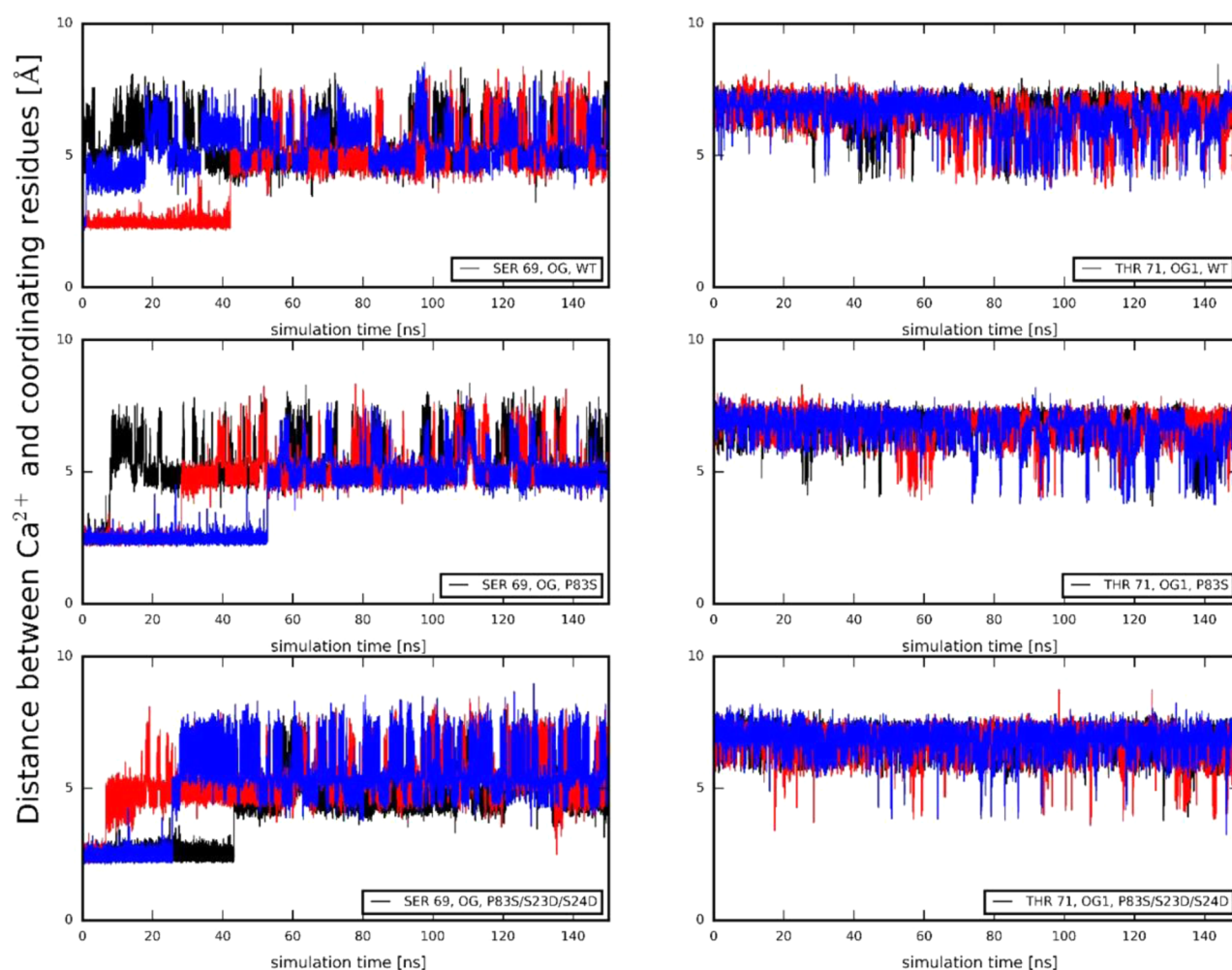


Figure 8. Distances between Ca^{2+} and its coordinating residue Ser-69 (left) and Thr-71 (right) of cTnC site II over the course of each MD simulation for WT, cTnI^{P83S}, and cTnI^{P83S/S23D/S24D} cTn systems. Here, the 1st run result is shown in black, the 2nd run result is in red, and the 3rd run result is in blue.

function. Figure 7A,B also highlights regions of cTn that play an important part in either Ca^{2+} binding (cTnC site I and cTnC site II) or cTnC–cTnI interaction (cTnI inhibitory-peptide and cTnI switch-peptide). In summary, cTnI^{P83S} had little impact on the dynamics of the troponin complex.

Next, we investigated the influence of PKA phosphorylation on cTn containing cTnI^{P83S}. To that end, we performed simulations with simultaneous phosphomimetic substitutions S23D and S24D and P83S of cTnI (cTnI^{P83S/S23D/S24D}) in the troponin structure. Figure 7C,D shows the average (\pm SD) RMSF of the cTnC and cTnI subunits for the cTnI^{P83S} and the cTnI^{P83S/S23D/S24D} systems. The fluctuations in the cTnI^{P83S/S23D/S24D} system were increased with respect to the cTnI^{P83S} system. Interestingly, there were increased dynamics in the entire structure of NcTnC, suggesting NcTnI mobility can have a profound influence on NcTnC dynamics. We also speculate that structural destabilization of cTnI (caused by the introduction of three amino acids substitutions) could be partially responsible for the wide range of RMSF values observed. The largest change of dynamical behavior between the two systems is observed in cTnI residues 20–30 where an increase in local residue fluctuations is observed. The Ser (S) to Asp (D) mutations break stabilizing interactions in the region, suggesting a large increase in the mobility of NcTnI. To better visualize how introduction of the P83S and/or bis-phosphomi-

mic substitutions influences the subunit interactions among the cTn complex, 15 snapshots taken from the entire MD simulations were superimposed (Figure 7E,F). For both structure alignments, cTnC is shown in blue, cTnI in red, and cTnT in yellow. In addition to the greater flexibility exhibited for the NcTnI in the cTnI^{S23D/S24D} cTn model with respect to the WT model, the introduction of S23D/S24D to the cTnI^{P83S} model also caused increased flexibility in NcTnC.

In addition to the change in entire protein dynamics/structures, we investigated how the cTnI^{P83S} mutation and/or PKA phosphorylation impact Ca^{2+} binding stability in site II. It is very difficult to accurately calculate binding affinities of Ca^{2+} , due to the nature of divalent cations. Therefore, we investigated one parameter related to the Ca^{2+} binding in site II in cTnC, the time evolution of distances between the bound Ca^{2+} ion and its coordinating residues. In the crystal structures, Ca^{2+} is coordinated with six atoms in cTnC site II residues: Asp-65 OD2, Asp-67 OD2, Ser-69 OG, Asp-73 OD2, Glu-76 OE1, and Glu-76 OE2. As observed in previous studies,^{34,35,39,62} the coordinating behavior of Asp-65, Asp-67, Asp-73, and Glu-76 did not change for WT cTn in the absence or presence of cTnI-S23D/S24D. The most interesting behavior is observed for Ser-69 OG and, perhaps, Thr-71 OG1. Figure 8 shows those distances over the time course of three independent 150 ns simulations for WT, cTnI^{P83S}, and cTnI^{P83S/S23D/S24D} cTn

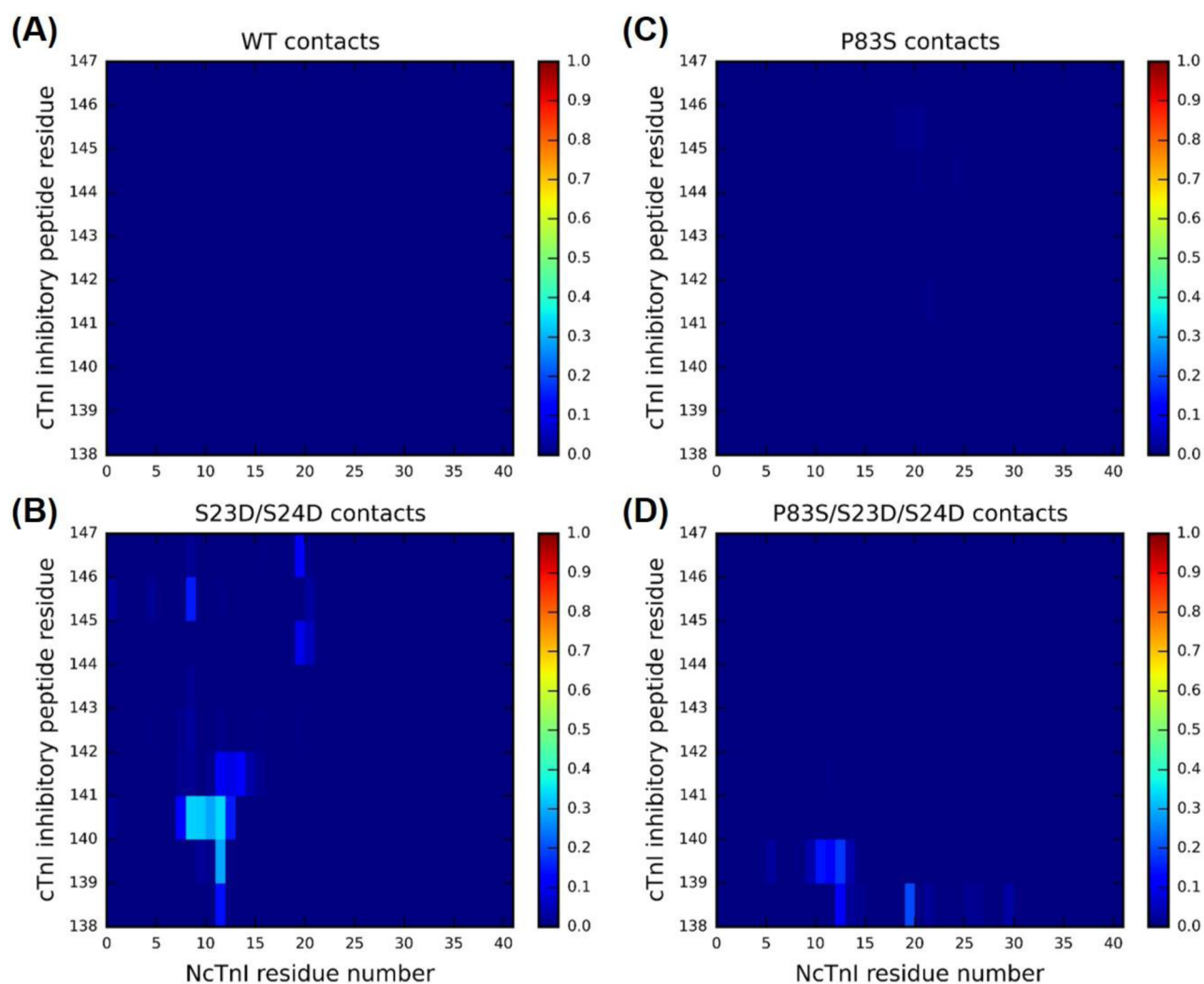


Figure 9. Average contact map of residue–residue pairs between the N-terminus (residues 1–41) and inhibitory-peptide region (residues 138–147) of cTnI for the (A) WT, (B) cTnI-S23D/S24D, (C) cTnI-P83S, and (D) cTnI-P83S/S23D/S24D cTn models. The blue end of the spectrum (value 0) reflects no contact within the residue–residue pair, while the red end of the spectrum (value 1) represents 100% contact within the residue–residue pair.

systems. The coordination behavior for both residues fluctuated over the course of the simulations for all three systems, in contrast to the stability of the other coordinating residues. Thr-71 generally does not coordinate, in agreement with structural data from X-ray crystallography. As demonstrated in Figure 8, the most pronounced difference between the simulations is observed in coordination of Ser-69, which is consistent with our previous observations.^{34,35,39,62} The percent-in-contact time of Ser-69 varies among the different systems. With respect to the WT system (10%), the percent-in-contact time is increased to 19% in the cTnI^{P83S} system, indicating a stronger interaction and a possible stabilization. This may interpret the increased Ca^{2+} binding affinity of cTnI^{P83S} with respect to the cTnI^{WT} observed from steady-state fluorescence measurements. Importantly, this contact time was not affected by introduction of the bis-phosphomimic substitutions (17% in the cTnI^{P83S/S23D/S24D} system), in agreement with the unchanged Ca^{2+} binding affinity (K_{Ca}) obtained from the steady-state fluorescence measurements.

Next, we monitored the residue–residue contacts of key regions during the time course of entire 450 ns simulations. We first focused on elucidating the intrasubunit contacts between

NcTnI (cTnI residues 1–41) and the cTnI inhibitory-peptide (cTnI residues 138–147). It has been previously shown that this may constitute an important mechanism by which PKA can regulate cTn structure and dynamics. The following interesting question arises: To what degree does the mutation cTnI^{P83S} impact that mechanism? We hypothesized that, due to its distance from NcTnI and the inhibitory-peptide, cTnI^{P83S} may not disrupt this mechanism that blunts PKA-mediated modulation of myofibril contraction and relaxation as much as other mutations (cTnI^{R21C} and cTnI^{R146G}).^{34,35} To this end, we examined intrasubunit contacts between NcTnI (cTnI residues 1–41) and the cTnI inhibitory-peptide (cTnI residues 138–147). Figure 9 shows the corresponding contact plots for (A) WT, (B) cTnI-S23D/S24D, (C) cTnI-P83S, and (D) cTnI-P83S/S23D/S24D, cTn complexes. As previously reported,⁶² there were no intrasubunit interactions between cTnI inhibitory-peptide and its N-terminus in the WT cTn system (see panel A), which changed dramatically with the cTnI^{S23D/S24D} substitutions where all three independent runs formed contacts between cTnI residues 9–14 and 140–142 for about 50% of the simulation time (panel B). No intrasubunit interactions were seen in the cTnI^{P83S} system (panel C), which

is not surprising since no phosphomimic substitutions or phosphorylations are present. As we expected, introduction of the cTnI^{P83S} mutation only moderately reduced the NcTnI–cTnI inhibitory-peptide interactions in the bis-phosphomimic system (cTnI^{P83S/S23D/S24D}, panel D). This suggests that interference with PKA regulation may be a mechanism (albeit not a strong one) of action of the cTnI^{P83S} mutation.

To further examine the region with direct contact between cTnC and cTnI with Ca²⁺ binding, we next studied the contact stability between the switch-peptide of cTnI (cTnI residues 148–164) and the 14 hydrophobic NcTnC residues (Phe-20, Ala-23, Phe-24, Ile-26, Phe-27, Ile-36, Leu-41, Val-44, Leu-48, Leu-57, Met-60, Phe-77, Met-80, and Met-81). Figure 10 displays the different contact maps of residue–residue pairs between those 14 hydrophobic residues of NcTnC and the cTnI switch-peptide for different systems. As we mentioned previously,³⁴ Ca²⁺ and the switch-peptide of cTnI were present at the beginning of the MD simulations (and we did not remove Ca²⁺ during MD simulations); thus, we did not expect to observe dramatic structural changes in this region. However, a variation in the contacts can be considered as an indicator of the cTnC–cTnI interaction (K_{C-I}) stability associated with activation. As compared with the WT cTn complex, there was some change in contact time upon introduction of the P83S mutant (panel A). A more dramatic change was seen upon introduction of the bis-phosphomimic substitutions to S23/S24 of the WT complex (cTnI-P83S/S23D/S24D), suggesting there was a decreased interaction between NcTnC hydrophobic residues and cTnI switch-peptide upon phosphorylation (panel B). With introduction of the bis-phosphomimic substitutions to the cTnI-P83S system (panel C), there was still some visible change in fluctuation for the contacts, but the degree (net change) of fluctuation is smaller than that for the WT complex. Together with the information for the intrasubunit contact of cTnI (Figure 9), our MD simulations suggest that phosphorylation of S23/S24 of cTnI results in the formation of an intrasubunit contact between cTnI inhibitory-peptide and NcTnI, which further reduces the stability of the interaction between cTnI switch-peptide and the cTnC hydrophobic-patch, and cTnI^{P83S} moderately abrogates this action. This suggests a potential structure-based mechanism of how cTnI^{P83S} may impair PKA regulation of contraction and relaxation.

DISCUSSION

cTnI^{P82S} (cTnI^{P83S} in rodents) has been considered as a potential disease-causing mutation,¹⁶ but others suggest it may be a benign polymorphic variant rather than a disease-causing one.¹⁷ Recently, Ramirez-Correa et al. demonstrated that cTnI^{P83S} resulted in mild diastolic dysfunction in aging mice.¹⁸ However, this mutation itself has not yet been reported to cause HCM in patients. So, it is of importance to study whether cTnI^{P82S} alters myofibril contractile properties, and whether the alterations of structural-function for cTnI^{P82S} are similar to other HCM-associated cTnI mutations. In this study, we characterized the effects of cTnI^{P83S} on structure–function relationship of cTn and on the contractile properties of rat left ventricular myofibrils, to compare with similar measurements made previously with other cTnI mutations that have been associated with HCM. Two HCM-associated mutations, cTnI^{R146G} and cTnI^{R21C} (located in the inhibitory-peptide and cardiac-specific N-terminus of cTnI, respectively), not only altered normal contractile properties, but also blunted the regulatory ability of PKA-mediated phosphorylation on S23/

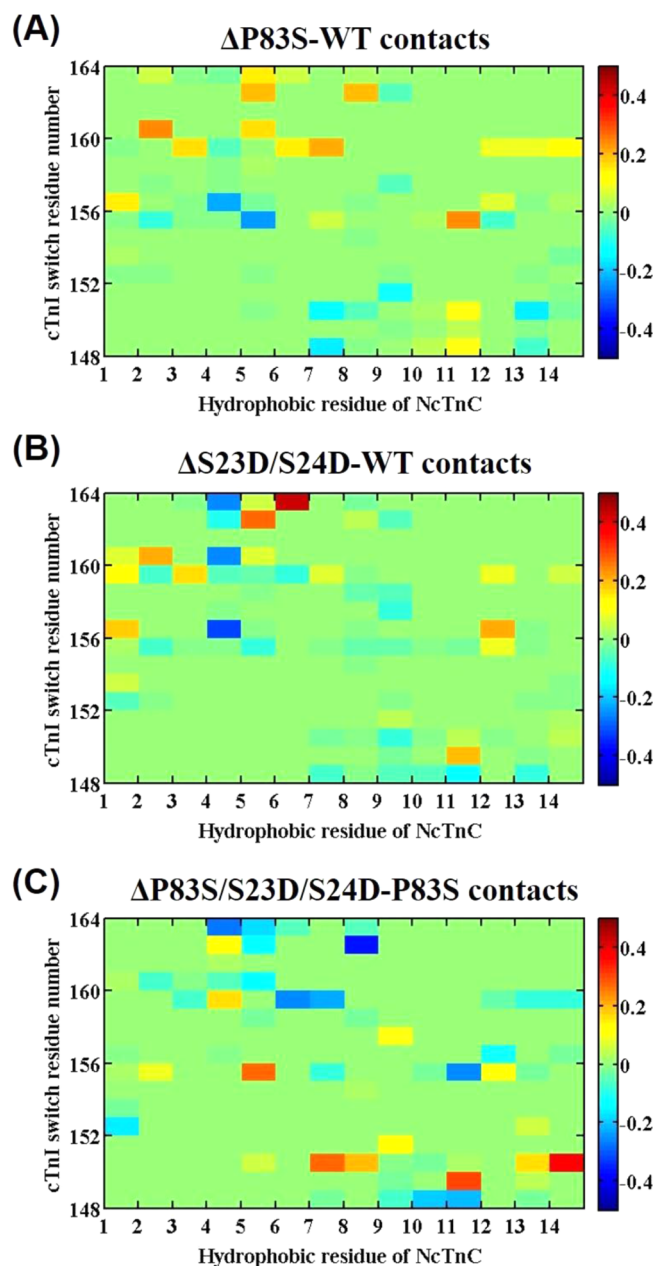


Figure 10. (A–C) Difference contact map of residue–residue pairs between 14 hydrophobic NcTnC residues and the switch-peptide of cTnI mostly affected upon introduction of mutation or the bis-phosphomimic substitutions. The 14 hydrophobic residues of NcTnC are the following (from left to right): Phe-20, Ala-23, Phe-24, Ile-26, Phe-27, Ile-36, Leu-41, Val-44, Leu-48, Leu-57, Met-60, Phe-77, Met-80, and Met-81. Color green (value 0) reflects no difference between the two systems; the red end of the spectrum (values above 0) reflects more contacts in the P83S (A), S23D/S24D (B), or P83S/S23D/S24D (C) cTn system, and the blue of the spectrum (values below 0) indicates more contacts in the WT (A), WT (B), or P83S (C) model.

S24 during β -adrenergic stimulation, and we attributed this to the disruption of the formation of an intrasubunit contact between cTnI inhibitory-peptide and NcTnI that is normally seen with phosphorylation.^{34,20} To understand whether these changes in contractile properties occur in all putative HCM cTnI mutations or are restricted to the mutations located in specific regions (such as N-terminus, inhibitory-peptide region), in this work, we studied the cTnI^{P83S} mutation that

is resided in the I–T arm region. The most significant findings for the current study were the following, compared to cTnI^{WT}: (1) cTnI^{P83S} increased both K_{Ca} and K_{C-I} , but may limit or eliminate the ability of S23/S24 phosphorylation to reduce these properties of cTn. (2) cTnI^{P83S} had no effect on T_{MAX} or the Ca^{2+} sensitivity of myofibril tension, but blunted PKA-phosphorylation-associated decrease in pCa_{50} . (3) cTnI^{P83S} at least partially blunted the PKA-mediated acceleration of the early, slow-phase of relaxation, and this may be correlated with moderate inhibition of an intrasubunit interaction between the cTnI inhibitory-peptide and NcTnI.

Comparison of cTnI^{P83S} with cTnI^{R146G} and cTnI^{R21C} Effects on cTn and Myofibril Function. T_{MAX} was maintained for cTnI^{P83S} exchanged myofibrils, as we previously observed for cTnI^{R146G} or cTnI^{R21C} exchanged myofibrils.³⁴ However, while the Ca^{2+} sensitivity of tension (pCa_{50}) was left-shifted by 0.13 or 0.10 pCa units for cTnI^{R146G} or cTnI^{R21C} exchanged myofibrils,³⁴ a left-shift of pCa_{50} was minimal (0.04 pCa units) and not statistically different ($P > 0.05$) for cTnI^{P83S} exchanged myofibrils. As we mentioned previously, C–I interaction serves as a “gatekeeper” in transmitting the Ca^{2+} signal to other myofilament proteins to initiate cardiac muscle contraction and tension development. Our myofibril results were in agreement with the steady-state fluorescence measurements where the K_{C-I} was left-shifted for cTnI^{P83S}; however, the extent of increment was smaller than those for cTnI^{R146G} and cTnI^{R21C}.³⁴ This result also correlated well with the steady-state cTn fluorescence measurements where the Ca^{2+} sensitivity of the fluorescence intensity increase (pCa_{50}) was only left-shifted 0.09 pCa units for cTnI^{P83S}, which is also smaller than those for cTn with cTnI^{R146G} (0.24 pCa units) or cTnI^{R21C} (0.22 pCa units).³⁴ Here, it is important to point out that the magnitude of pCa_{50} change (increment or decrease) is variant in different systems, such as the net change of pCa_{50} for Ca^{2+} sensitivity of tension was smaller than those in the steady-state Ca^{2+} –cTn binding. To understand its structural basis, we monitored the time-evolution of distances between the Ca^{2+} ion (site-II) and its six coordinating residues over the time course of total 450 ns MD simulations. The percent-in-contact time can partially act as an indicator to suggest a strong interaction and a possible stabilization with Ca^{2+} . We found that coordination of Ser-69 with Ca^{2+} was increased to 19% for cTnI^{P83S} mutation (Figure 7), a smaller value than that for either cTnI^{R146G} (29%) or cTnI^{R21C} (23%), which is consistent with our steady-state Ca^{2+} –cTn binding affinity measurement.^{34,35} Taken together, these results suggest cTnI^{P83S} behaves midway between two severe HCM-associated cTnI mutations and WT cTnI, suggesting it has a more moderate effect on cTn function.

The effect of cTnI^{P83S} on myofibril activation was similar to what we have reported for cTnI^{R146G} and cTnI^{R21C}. When comparing the Ca^{2+} -dependent thin filament activation protocol (k_{ACT}) with the rapid release–restretch protocol (k_{TR}) for the same activation trial, k_{TR} was faster than k_{ACT} at all Ca^{2+} levels we tested, for both cTnI^{WT} and cTnI^{P83S} exchanged myofibrils (at 15 °C). This result is in accordance with our previous observations in rodent (and canine) heart.^{10,34,49,54} However, it is different from several other reports of no difference between k_{ACT} and k_{TR} ^{63,67} and we have demonstrated that this is due to the lack of a phosphate mop in our solutions, which results in the presence of 0.5 mM P_i (a level of P_i that is close to the physiological level of P_i present in the heart) in our solutions.¹⁰ The presence of P_i specifically

influences the cross-bridge tension generating isomerization, and not affecting the kinetics for thin filament activation.⁴⁹ Thus, all three mutations do not appear to affect the thin filament activation kinetics in the absence of β -adrenergic stimulation.

During the slow-phase relaxation, subsequent to rapid reduction in Ca^{2+} , the sarcomeres still maintain in isometric conditions, such that the tension decays with a linear, constant rate. Thus, $k_{REL,slow}$ monitors the turnover kinetics of cross-bridge cycling, dominated by the detachment rate.^{49,53,63–66} The slow-phase of relaxation duration ($t_{REL,slow}$) depends on the Ca^{2+} activation levels and can be affected by Ca^{2+} –cTn binding and, likely, the cTnC–cTnI interaction properties of cTn.⁶⁷ Both $k_{REL,slow}$ and $t_{REL,slow}$ were not affected by the cTnI^{P83S} mutation, at either maximal and submaximal levels of Ca^{2+} activation. This result is different than what we previously observed on cTnI^{R146G} and cTnI^{R21C} exchanged myofibrils, with both significantly prolonged $t_{REL,slow}$ again suggesting cTnI^{P83S} has more moderate effects.

Additional comparisons were made between the three mutations in the ability to affect PKA modulation of cTn function, and the contractile properties of myofibrils. PKA treatment of cTnI^{WT} exchanged myofibrils right-shifted pCa_{50} (~0.18 pCa units), and this effect was eliminated with cTnI^{P83S} (Figure 5B). Additionally, the k_{ACT}/k_{TR} ratio was decreased from 0.67 to 0.52 for cTnI^{WT} exchanged myofibrils upon PKA treatment, suggesting a slowed thin filament activation process. Interestingly, the k_{ACT}/k_{TR} ratio did not differ with PKA phosphorylation for cTnI^{P83S}, which is similar to what we reported for cTnI^{R146G} and cTnI^{R21C}. Also similar was the observation that cTnI^{P83S} blunted the ability of PKA to speed the early, slow-phase of myofibril relaxation (Figure 6). Using steady-state fluorescence measurements, we found that introduction of the bis-phosphomimic substitutions on cTnI resulted in a quite similar reduction of the Ca^{2+} binding affinity to cTn (K_{Ca}) for all complexes (except cTnI^{P83S}). However, the decrease of C–I interaction (K_{C-I}) observed in cTnI^{WT} did not occur for all three cTnI mutations. Those findings suggest that it may be the alteration of C–I interaction *per se* that perturbs (blunt) the modulation of PKA-mediated phosphorylation (on S23/S24 of cTnI) on altering the contractile properties for at least some cTnI mutations associated with HCM. It is of importance to point out that, in regard to the steady-state C–I binding measurements (in the presence of Ca^{2+}), there are at least two kinds of C–I interactions (the hydrophobic batch of cTnC with switch-peptide of cTnI, and the cTnC with the N-terminus of cTnI, etc). We also measured the C–I binding in the absence of Ca^{2+} (date not present), and the K_{C-I} values were saturated more slowly and were right-shifted (compared to the presence of Ca^{2+} condition) for all cTnI variants. In the absence of Ca^{2+} , the regulatory domain of cTnC was in the closed conformation, and cTnI may just nonspecifically bind to cTnC, such that the C–I binding without Ca^{2+} is not a good indicator. On the other hand, the presence of Ca^{2+} induces an “open” confirmation of the NcTnC, and allows the hydrophobic-patch of cTnC to interact with the switch-peptide of cTnI. Together, although it is hard to only measure the C–I binding between the hydrophobic-patch of cTnC with the switch-peptide of cTnI, it is the primary C–I binding portion in the presence of Ca^{2+} . Additionally, the presence of Ca^{2+} is relevant to the physiology conditions that lead to muscle contraction and tension production.

Interestingly, the blunted or abnormal cardiac response to β -adrenergic stimulation had also been reported for several other cardiomyopathy mutations.^{19,69–75} For example, Li et al. and Schmidtmann et al. found that the cTnC^{L29Q} mutation hindered the effect of PKA-mediated phosphorylation of cTnI on transducing the signal from cTnC to cTnI, and Dong et al. reported that this mutation blunted the enhancement of NcTnC closing rate upon cTnI phosphorylation by PKA.^{70–72} Using the *in vitro* motility assay, Deng et al. reported that cTnI^{R145G} mutation suppressed the PKA effects on the maximal *in vitro* sliding velocity and maximal actoS1-ATPase activity.¹⁹ By exchanging the cTn complex into skinned rat trabeculae, Biesiadecki et al. found that cTnC^{G159D} mutation blunted the PKA phosphorylation induced decrease in the Ca^{2+} sensitivity of tension development (pCa_{50}).⁶⁹ Using an *in vitro* motility assay, Messer et al. reported that seven HCM-associated mutations in cTnT uncoupled the modulation of Ca^{2+} sensitivity by PKA phosphorylation of cTnI.⁷³ To mimic PKA phosphorylation, we built up a bis-phosphomimic (cTnI^{S23D/S24D} cTn) model by mutating the S23/S24 of cTnI to aspartic acid (D). Despite the charge and molecular space of real phosphorylation and the phosphorylation mimetics being different, the cTnI^{S23D/S24D} substitution has previously been demonstrated to mimic the effects of PKA phosphorylation on S23/S24 of cTnI (cTnI^{pS23/pS24}) both structurally and functionally.^{76–79} Finley et al. found that cTnI^{(1–80) DD}, which had phosphorylated serine residues mutated to aspartic acid, served as a good structural mimetic of the phosphorylated state and would facilitate future biophysical studies.⁷⁶ Following this, several groups (including ours) have used the cTnI^{S23D/S24D} substitution instead of the cTnI^{pS23/pS24} to study the effects of PKA-mediated phosphorylation on cardiac function, as it serves as a useful tool to study the specific effect of PKA-mediated phosphorylation of cTnI, in the absence of cMyBP-C and titin phosphorylation that also occurs during β -adrenergic stimulation.^{80,81} As we reported previously, introduction of the bis-phosphomimic substitutions at S23/S24 led to the formation of an intrasubunit interaction between the N-terminus and the inhibitory-peptide regions of cTnI for WT cTn simulations,⁶² which has been previously proposed by Solaro et al. based on the spectroscopic and solution biochemistry measurements.^{13,56,82} Additionally, our simulation results suggested a bending at the N-terminus of cTnI and the formation of a more compact cTn structure with the introduction of bis-phosphomimic substitutions (on WT-cTn), which is in accordance with the biochemical studies by several other laboratories.^{83–85} Interestingly, this intrasubunit interaction no longer occurs in the presence of either cTnI^{R146G} or cTnI^{R21C}. This result was not surprising since these mutations are located in the interacting regions, either the inhibitory-peptide (cTnI^{R146G}) or N-terminus (cTnI^{R21C}) of cTnI, which may directly inhibit the formation of intrasubunit contacts between these two regions. However, cTnI^{P83S} resides in the I–T arm of cTnI and does not directly interact with either region. Thus, our finding that there is still a moderate amount of intrasubunit interaction (though reduced) makes sense and may explain the lesser influence of cTnI^{P83S} (compared with cTnI^{R146G} or cTnI^{R21C}) in blunting PKA-mediated modulation of function. Our findings may at least partially explain the contradictory reports and conclusions in the literature of cTnI^{P82S}. Taken together, it suggests that cTnI^{P82S} could contribute to a hypertrophic phenotype in the heart, but it would likely require an additional causal genetic mutation or epigenetic conditions.

This is correlated to what Frazier et al. reported previously, in which an African American individual with severe HCM had identified mutations both in cTnI^{P82S} and MYH7^{R453S}.¹⁷

Finally, there are some limitations present in the current study, such as the following: (1) We did not do protein studies looking at the interaction of the N-terminal extension of cTnI with the inhibitory-peptide. This would have to be done with NMR and would have its own limitations because you cannot study whole cTn with NMR. (2) We did not measure Ca^{2+} dissociation rate or cTnC–cTnI interaction in myofibrils. For exploring a future direction, we can introduce some techniques (such as FRET) to our myofibril mechanics/kinetics setup, thus allowing us to collect the kinetics results accompanied with the information related to structural alteration.

CONCLUSION

The cardiac troponin (cTn) complex plays a pivotal regulatory role in myofilament contraction and tension generation. Studying how disease-related mutations affect conformational changes in cTn provides insight as to how Ca^{2+} -mediated signal transduction may be altered and may result in contractile dysfunction associated with cardiac disease (the correlations between genotype and phenotype). Recently, we reported the altered structure–function relationship for two HCM-associated cTnI mutations, located in either the inhibitory-peptide (cTnI^{R146G}) or cardiac-specific N-terminus of cTnI (cTnI^{R21C}).^{34,35} Our results suggested that the structural basis of how both mutations blunted the ability of PKA-mediated phosphorylation to modulate both contraction and relaxation is prohibiting the formation of an intrasubunit interaction between the inhibitory-peptide and N-terminus of cTnI.^{34,35} Here, we expanded this information to a mutation (cTnI^{P83S}) that is not located in those specific regions, and the possible (potential) mechanism of how this mutant may alter the cardiac function. Our findings also partially explain the contradictory reports of cTnI^{P82S} in the literature, and proposed that cTnI^{P82S} possibly requires additional conditions to contribute to a hypertrophic phenotype in the heart. Taken together, the combination of experimental (such as solution protein biochemistry, myofibril mechanic and kinetics measurements) and computational (MD simulations) approaches provides a powerful interdisciplinary to understand the molecular mechanisms of how disease-related mutations (and PKA-mediated phosphorylation on myofilament proteins during β -adrenergic stimulation) affect the structure–function relationship.

AUTHOR INFORMATION

Corresponding Author

*E-mail: mregnier@uw.edu.

Notes

The authors declare no competing financial interest.

ACKNOWLEDGMENTS

We would like to express our special appreciation of Prof. J. Andrew McCammon for his mentoring, advice, and support of this work. Prof. Rommie Amaro is the director of National Biochemical Computation Resource (NBCR), and we appreciate her support of this work. We thank Drs. Maria Razumova and Galina Flint for the assistance with rat tissue and solution preparation. We appreciate Drs. John Solaro and Paul Rosevear for structural information on the cTnI N-terminal extension.

We are indebted to Martha Mathiason for data acquisition and analysis software development. M.R. is an Established Investigator of the American Heart Association (AHA). This research was supported by NIH R01 HL-111197 (M.R.), and AHA 15POST25080292 (Y.C.). Funding and support from the NBCR is provided through NIH P41 GM103426. Work in the JAM group is partially supported by NSF, NIH, HHMI, and the NSF Supercomputer Centers.

REFERENCES

- (1) Maron, B. J.; Gardin, J. M.; Flack, J. M.; Gidding, S. S.; Kurosaki, T. T.; Bild, D. E. Prevalence of Hypertrophic Cardiomyopathy in a General-Population of Young-Adults - Echocardiographic Analysis of 4111 Subjects in the Cardia Study. *Circulation* **1995**, *92*, 785–789.
- (2) Elliott, P.; Andersson, B.; Arbustini, E.; Bilinska, Z.; Cecchi, F.; Charron, P.; Dubourg, O.; HL, U. K. R.; Maisch, B.; McKenna, W. J.; et al. Classification of the Cardiomyopathies: A Position Statement from the European Society of Cardiology Working Group on Myocardial and Pericardial Diseases. *Eur. Heart J.* **2008**, *29*, 270–276.
- (3) Mogensen, J.; Murphy, R. T.; Kubo, T.; Bahl, A.; Moon, J. C.; Klausen, I. C.; Elliott, P. M.; McKenna, W. J. Frequency and Clinical Expression of Cardiac Troponin I Mutations in 748 Consecutive Families with Hypertrophic Cardiomyopathy. *J. Am. Coll. Cardiol.* **2004**, *44*, 2315–2325.
- (4) Tester, D. J.; Ackerman, M. J. Cardiomyopathic and Channelopathic Causes of Sudden Unexplained Death in Infants and Children. *Annu. Rev. Med.* **2009**, *60*, 69–84.
- (5) Willott, R. H.; Gomes, A. V.; Chang, A. N.; Parvatiyar, M. S.; Pinto, J. R.; Potter, J. D. Mutations in Troponin That Cause Hcm, Dcm and Rcm: What Can We Learn About Thin Filament Function? *J. Mol. Cell. Cardiol.* **2010**, *48*, 882–892.
- (6) Gordon, A. M.; Homsher, E.; Regnier, M. Regulation of Contraction in Striated Muscle. *Physiol. Rev.* **2000**, *80*, 853–924.
- (7) Dong, W. J.; Xing, J.; Villain, M.; Hellinger, M.; Robinson, J. M.; Chandra, R.; Solaro, R. J.; Umeda, P. K.; Cheung, H. C. Conformation of the Regulatory Domain of Cardiac Muscle Troponin C in Its Complex with Cardiac Troponin I. *J. Biol. Chem.* **1999**, *274*, 31382–31390.
- (8) Spyrapopoulos, L.; Li, M. X.; Sia, S. K.; Gagne, S. M.; Chandra, M.; Solaro, R. J.; Sykes, B. D. Calcium-Induced Structural Transition in the Regulatory Domain of Human Cardiac Troponin C. *Biochemistry* **1997**, *36*, 12138–12146.
- (9) Zhang, R.; Zhao, J.; Mandveno, A.; Potter, J. D. Cardiac Troponin I Phosphorylation Increases the Rate of Cardiac Muscle Relaxation. *Circ. Res.* **1995**, *76*, 1028–1035.
- (10) Rao, V.; Cheng, Y. H.; Lindert, S.; Wang, D.; Oxenford, L.; McCulloch, A. D.; McCammon, J. A.; Regnier, M. Pka Phosphorylation of Cardiac Troponin I Modulates Activation and Relaxation Kinetics of Ventricular Myofibrils. *Biophys. J.* **2014**, *107*, 1196–1204.
- (11) Chandra, M.; Dong, W.-J.; Pan, B.-S.; Cheung, H. C.; Solaro, R. J. Effects of Protein Kinase A Phosphorylation on Signaling between Cardiac Troponin I and the N-Terminal Domain of Cardiac Troponin C. *Biochemistry* **1997**, *36*, 13305–13311.
- (12) Kentish, J. C.; McCloskey, D. T.; Layland, J.; Palmer, S.; Leiden, J. M.; Martin, A. F.; Solaro, R. J. Phosphorylation of Troponin I by Protein Kinase A Accelerates Relaxation and Crossbridge Cycle Kinetics in Mouse Ventricular Muscle. *Circ. Res.* **2001**, *88*, 1059–1065.
- (13) Solaro, R. J.; Rosevear, P.; Kobayashi, T. The Unique Functions of Cardiac Troponin I in the Control of Cardiac Muscle Contraction and Relaxation. *Biochem. Biophys. Res. Commun.* **2008**, *369*, 82–87.
- (14) Kimura, A.; Harada, H.; Park, J. E.; Nishi, H.; Satoh, M.; Takahashi, M.; Hiroi, S.; Sasaoka, T.; Ohbuchi, N.; Nakamura, T.; et al. Mutations in the Cardiac Troponin I Gene Associated with Hypertrophic Cardiomyopathy. *Nat. Genet.* **1997**, *16*, 379–382.
- (15) Cheng, Y.; Regnier, M. Cardiac Troponin Structure-Function and the Influence of Hypertrophic Cardiomyopathy Associated Mutations on Modulation of Contractility. *Arch. Biochem. Biophys.* **2016**, DOI: 10.1016/j.abb.2016.02.004.
- (16) Niimura, H.; Patton, K. K.; McKenna, W. J.; Soult, J.; Maron, B. J.; Seidman, J. G.; Seidman, C. E. Sarcomere Protein Gene Mutations in Hypertrophic Cardiomyopathy of the Elderly. *Circulation* **2002**, *105*, 446–451.
- (17) Frazier, A.; Judge, D. P.; Schulman, S. P.; Johnson, N.; Holmes, K. W.; Murphy, A. M. Familial Hypertrophic Cardiomyopathy Associated with Cardiac Beta-Myosin Heavy Chain and Troponin I Mutations. *Pediatr. Cardiol.* **2008**, *29*, 846–850.
- (18) Ramirez-Correa, G. A.; Frazier, A. H.; Zhu, G. S.; Zhang, P. B.; Rappold, T.; Kooij, V.; Bedja, D.; Snyder, G. A.; Lugo-Fagundo, N. S.; Hariharan, R.; et al. Cardiac Troponin I Pro82ser Variant Induces Diastolic Dysfunction, Blunts Beta-Adrenergic Response, and Impairs Myofilament Cooperativity. *J. Appl. Physiol.* **2015**, *118*, 212–223.
- (19) Deng, Y.; Schmidtman, A.; Redlich, A.; Westerdorf, B.; Jaquet, K.; Thieleczek, R. Effects of Phosphorylation and Mutation R145G on Human Cardiac Troponin I Function. *Biochemistry* **2001**, *40*, 14593–14602.
- (20) Lang, R.; Gomes, A. V.; Zhao, J. J.; Housmans, P. R.; Miller, T.; Potter, J. D. Functional Analysis of a Troponin I (R145G) Mutation Associated with Familial Hypertrophic Cardiomyopathy. *J. Biol. Chem.* **2002**, *277*, 11670–11678.
- (21) Lindhout, D. A.; Li, M. X.; Schieve, D.; Sykes, B. D. Effects of T142 Phosphorylation and Mutation R145G on the Interaction of the Inhibitory Region of Human Cardiac Troponin I with the C-Domain of Human Cardiac Troponin C. *Biochemistry* **2002**, *41*, 7267–7274.
- (22) Westfall, M. V.; Borton, A. R.; Albayya, F. P.; Metzger, J. M. Myofilament Calcium Sensitivity and Cardiac Disease-Insights from Troponin I Isoforms and Mutants. *Circ. Res.* **2002**, *91*, S25–S31.
- (23) Elliott, K.; Watkins, H.; Redwood, C. S. Altered Regulatory Properties of Human Cardiac Troponin I Mutants That Cause Hypertrophic Cardiomyopathy. *J. Biol. Chem.* **2000**, *275*, 22069–22074.
- (24) Takahashi-Yanaga, F.; Morimoto, S.; Harada, K.; Minakami, R.; Shiraiishi, F.; Ohta, M.; Lu, U. W.; Sasaguri, T.; Ohtsuki, I. Functional Consequences of the Mutations in Human Cardiac Troponin I Gene Found in Familial Hypertrophic Cardiomyopathy. *J. Mol. Cell. Cardiol.* **2001**, *33*, 2095–2107.
- (25) Reis, S.; Littwitz, C.; Preilowski, S.; Mugge, A.; Stienen, G. J. M.; Pott, L.; Jaquet, K. Expression of cTnI-R145G Affects Shortening Properties of Adult Rat Cardiomyocytes. *Pfluegers Arch.* **2008**, *457*, 17–24.
- (26) Wen, Y. H.; Pinto, J. R.; Gomes, A. V.; Xu, Y. Y.; Wang, Y. C.; Wang, Y.; Potter, J. D.; Kerrick, W. G. L. Functional Consequences of the Human Cardiac Troponin I Hypertrophic Cardiomyopathy Mutation R145G in Transgenic Mice. *J. Biol. Chem.* **2008**, *283*, 20484–20494.
- (27) Kruger, M.; Zittich, S.; Redwood, C.; Blaudeck, N.; James, J.; Robbins, J.; Pfitzer, G.; Stehle, R. Effects of the Mutation R145G in Human Cardiac Troponin I on the Kinetics of the Contraction-Relaxation Cycle in Isolated Cardiac Myofibrils. *J. Physiol.* **2005**, *564*, 347–357.
- (28) Kobayashi, T.; Solaro, R. J. Increased Ca^{2+} Affinity of Cardiac Thin Filaments Reconstituted with Cardiomyopathy-Related Mutant Cardiac Troponin I. *J. Biol. Chem.* **2006**, *281*, 13471–13477.
- (29) Zhou, Z. Q.; Rieck, D.; Li, K. L.; Ouyang, Y. X.; Dong, W. J. Structural and Kinetic Effects of Hypertrophic Cardiomyopathy Related Mutations R146G/Q and R163W on the Regulatory Switching Activity of Rat Cardiac Troponin I. *Arch. Biochem. Biophys.* **2013**, *535*, 56–67.
- (30) Brunet, N. M.; Chase, P. B.; Mihajlovic, G.; Schoffstall, B. Ca^{2+} -Regulatory Function of the Inhibitory Peptide Region of Cardiac Troponin I Is Aided by the C-Terminus of Cardiac Troponin T: Effects of Familial Hypertrophic Cardiomyopathy Mutations Ctni R145g and Ctnt R278c, Alone and in Combination, on Filament Sliding. *Arch. Biochem. Biophys.* **2014**, *552*, 11–20.
- (31) Gomes, A. V.; Harada, K.; Potter, J. D. A Mutation in the N-Terminus of Troponin I That Is Associated with Hypertrophic Cardiomyopathy Affects the Ca^{2+} -Sensitivity, Phosphorylation Kinetics

and Proteolytic Susceptibility of Troponin. *J. Mol. Cell. Cardiol.* **2005**, *39*, 754–765.

(32) Wang, Y. C.; Pinto, J. R.; Solis, R. S.; Dweck, D.; Liang, J. S.; Diaz-Perez, Z.; Ge, Y.; Walker, J. W.; Potter, J. D. Generation and Functional Characterization of Knock-in Mice Harboring the Cardiac Troponin I-R21C Mutation Associated with Hypertrophic Cardiomyopathy. *J. Biol. Chem.* **2012**, *287*, 2156–2167.

(33) Dweck, D.; Sanchez-Gonzalez, M. A.; Chang, A. N.; Dulce, R. A.; Badger, C. D.; Koutnik, A. P.; Ruiz, E. L.; Griffin, B.; Liang, J. S.; Kabbaj, M.; et al. Long Term Ablation of Protein Kinase a (PKA)-Mediated Cardiac Troponin I Phosphorylation Leads to Excitation-Contraction Uncoupling and Diastolic Dysfunction in a Knock-in Mouse Model of Hypertrophic Cardiomyopathy. *J. Biol. Chem.* **2014**, *289*, 23097–23111.

(34) Cheng, Y.; Rao, V.; Tu, A.-y.; Lindert, S.; Wang, D.; Oxenford, L.; McCulloch, A. D.; McCammon, J. A.; Regnier, M. Troponin I Mutations R146G and R21C Alter Cardiac Troponin Function, Contractile Properties, and Modulation by Protein Kinase a (PKA)-Mediated Phosphorylation. *J. Biol. Chem.* **2015**, *290*, 27749–27766.

(35) Lindert, S.; Cheng, Y. H.; Kekenus-Huskey, P.; Regnier, M.; McCammon, J. A. Effects of Hcm Ctni Mutation R145G on Troponin Structure and Modulation by Pka Phosphorylation Elucidated by Molecular Dynamics Simulations. *Biophys. J.* **2015**, *108*, 395–407.

(36) Köhler, J.; Chen, Y.; Brenner, B.; Gordon, A. M.; Kraft, T.; Martyn, D. A.; Regnier, M.; Rivera, A. J.; Wang, C.-K.; Chase, P. B. Familial Hypertrophic Cardiomyopathy Mutations in Troponin I (K183Δ, G203S, K206Q) Enhance Filament Sliding. *Physiol. Genomics* **2003**, *14*, 117–128.

(37) Gordon, A. M.; Qian, Y.; Luo, Z.; Wang, C. K.; Mondares, R. L.; Martyn, D. A. Characterization of Troponin-C Interactions in Skinned Barnacle Muscle: Comparison with Troponin-C from Rabbit Striated Muscle. *J. Muscle Res. Cell Motil.* **1997**, *18*, 643–653.

(38) Martyn, D. A.; Regnier, M.; Xu, D.; Gordon, A. M. Ca²⁺- and Cross-Bridge-Dependent Changes in N- and C-Terminal Structure of Troponin C in Rat Cardiac Muscle. *Biophys. J.* **2001**, *80*, 360–370.

(39) Wang, D.; Robertson, I. M.; Li, M. X.; McCully, M. E.; Crane, M. L.; Luo, Z.; Tu, A.-Y.; Daggett, V.; Sykes, B. D.; Regnier, M. Structural and Functional Consequences of the Cardiac Troponin C L48Q Ca²⁺-Sensitizing Mutation. *Biochemistry* **2012**, *51*, 4473–4487.

(40) Wang, D.; McCully, M. E.; Luo, Z.; McMichael, J.; Tu, A.-Y.; Daggett, V.; Regnier, M. Structural and Functional Consequences of Cardiac Troponin C L57Q and I61Q Ca²⁺-Desensitizing Variants. *Arch. Biochem. Biophys.* **2013**, *535*, 68–75.

(41) Potter, J. D. Preparation of Troponin and Its Subunits. *Methods Enzymol.* **1982**, *85*, 241–263.

(42) Dong, W.-J.; Robinson, J. M.; Stagg, S.; Xing, J.; Cheung, H. C. Ca²⁺-Induced Conformational Transition in the Inhibitory and Regulatory Regions of Cardiac Troponin I. *J. Biol. Chem.* **2003**, *278*, 8686–8692.

(43) Patton, C.; Thompson, S.; Epel, D. Some Precautions in Using Chelators to Buffer Metals in Biological Solutions. *Cell Calcium* **2004**, *35*, 427–431.

(44) George, S. E.; Su, Z.; Fan, D.; Wang, S.; Johnson, J. D. The Fourth Ef-Hand of Calmodulin and Its Helix–Loop–Helix Components: Impact on Calcium Binding and Enzyme Activation. *Biochemistry* **1996**, *35*, 8307–8313.

(45) Adhikari, B. B.; Regnier, M.; Rivera, A. J.; Kreutziger, K. L.; Martyn, D. A. Cardiac Length Dependence of Force and Force Redevelopment Kinetics with Altered Cross-Bridge Cycling. *Biophys. J.* **2004**, *87*, 1784–1794.

(46) Regnier, M.; Rivera, A. J.; Chen, Y.; Chase, P. B. 2-Deoxy-ATP Enhances Contractility of Rat Cardiac Muscle. *Circ. Res.* **2000**, *86*, 1211–1217.

(47) Brenner, B.; Eisenberg, E. Rate of Force Generation in Muscle: Correlation with Actomyosin Atpase Activity in Solution. *Proc. Natl. Acad. Sci. U. S. A.* **1986**, *83*, 3542–3546.

(48) Fabiato, A. Computer Programs For Calculating Total From Specified Free Or Free From Specified Total Ionic Concentrations In

Aqueous Solutions Containing Multiple Metals And Ligands. *Methods Enzymol.* **1988**, *157*, 378–417.

(49) Kreutziger, K. L.; Piroddi, N.; McMichael, J. T.; Tesi, C.; Poggesi, C.; Regnier, M. Calcium Binding Kinetics of Troponin C Strongly Modulate Cooperative Activation and Tension Kinetics in Cardiac Muscle. *J. Mol. Cell. Cardiol.* **2011**, *50*, 165–174.

(50) Colomo, F.; Piroddi, N.; Poggesi, C.; te Kronnie, G.; Tesi, C. Active and Passive Forces of Isolated Myofibrils from Cardiac and Fast Skeletal Muscle of the Frog. *J. Physiol.* **1997**, *500*, 535–548.

(51) Racca, A. W.; Beck, A. E.; McMillin, M. J.; Korte, F. S.; Bamshad, M. J.; Regnier, M. The Embryonic Myosin R672C Mutation That Underlies Freeman-Sheldon Syndrome Impairs Cross-Bridge Detachment and Cycling in Adult Skeletal Muscle. *Hum. Mol. Genet.* **2015**, *24*, 3348–3358.

(52) Tesi, C.; Colomo, F.; Nencini, S.; Piroddi, N.; Poggesi, C. The Effect of Inorganic Phosphate on Force Generation in Single Myofibrils from Rabbit Skeletal Muscle. *Biophys. J.* **2000**, *78*, 3081–3092.

(53) Kreutziger, K. L.; Piroddi, N.; Scellini, B.; Tesi, C.; Poggesi, C.; Regnier, M. Thin Filament Ca²⁺ Binding Properties and Regulatory Unit Interactions Alter Kinetics of Tension Development and Relaxation in Rabbit Skeletal Muscle. *J. Physiol.* **2008**, *586*, 3683–3700.

(54) Cheng, Y.; Hogarth, K. A.; O'Sullivan, M. L.; Regnier, M.; Pyle, W. G. 2-Deoxyadenosine Triphosphate Restores the Contractile Function of Cardiac Myofibril from Adult Dogs with Naturally Occurring Dilated Cardiomyopathy. *Am. J. Physiol-Heart. Circ. Physiol.* **2016**, *310*, H80–H91.

(55) Takeda, S.; Yamashita, A.; Maeda, K.; Maeda, Y. Structure of the Core Domain of Human Cardiac Troponin in the Ca²⁺-Saturated Form. *Nature* **2003**, *424*, 35–41.

(56) Howarth, J. W.; Meller, J.; Solaro, R. J.; Trewhella, J.; Rosevear, P. R. Phosphorylation-Dependent Conformational Transition of the Cardiac Specific N-Extension of Troponin I in Cardiac Troponin. *J. Mol. Biol.* **2007**, *373*, 706–722.

(57) Humphrey, W.; Dalke, A.; Schulten, K. Vmd: Visual Molecular Dynamics. *J. Mol. Graphics* **1996**, *14*, 33–38.

(58) Jorgensen, W. L.; Chandrasekhar, J.; Madura, J. D.; Impey, R. W.; Klein, M. L. Comparison of Simple Potential Functions for Simulating Liquid Water. *J. Chem. Phys.* **1983**, *79*, 926–935.

(59) Phillips, J. C.; Braun, R.; Wang, W.; Gumbart, J.; Tajkhorshid, E.; Villa, E.; Chipot, C.; Skeel, R. D.; Kale, L.; Schulten, K. Scalable Molecular Dynamics with NAMD. *J. Comput. Chem.* **2005**, *26*, 1781–1802.

(60) MacKerell, A. D.; Banavali, N.; Foloppe, N. Development and Current Status of the Charmm Force Field for Nucleic Acids. *Biopolymers* **2000**, *56*, 257–265.

(61) Ryckaert, J.-P.; Ciccotti, G.; Berendsen, H. J. C. Numerical Integration of the Cartesian Equations of Motion of a System with Constraints: Molecular Dynamics of N-Alkanes. *J. Comput. Phys.* **1977**, *23*, 327–341.

(62) Cheng, Y. H.; Lindert, S.; Kekenus-Huskey, P.; Rao, V. S.; Solaro, R. J.; Rosevear, P. R.; Amaro, R.; McCulloch, A. D.; McCammon, J. A.; Regnier, M. Computational Studies of the Effect of the S23d/S24d Troponin I Mutation on Cardiac Troponin Structural Dynamics. *Biophys. J.* **2014**, *107*, 1675–1685.

(63) Poggesi, C.; Tesi, C.; Stehle, R. Sarcomeric Determinants of Striated Muscle Relaxation Kinetics. *Pfluegers Arch.* **2005**, *449*, 505–517.

(64) Kress, M.; Huxley, H. E.; Faruqi, A. R.; Hendrix, J. Structural Changes During Activation of Frog Muscle Studied by Time-Resolved X-Ray Diffraction. *J. Mol. Biol.* **1986**, *188*, 325–342.

(65) Huxley, A. F.; Simmons, R. M. Rapid 'Give' and the Tension 'Shoulder' in the Relaxation of Frog Muscle Fibres. *J. Physiol.* **1970**, *210*, 32P–33P.

(66) Luo, Y.; Davis, J.; Tikunova, S.; Smillie, L.; Rall, J. Myofibrillar Determinants of Rate of Relaxation in Skinned Skeletal Muscle Fibers. In *Molecular and Cellular Aspects of Muscle Contraction*; Sugi, H., Ed.; Springer, 2003; Vol. 538, Chapter 51, pp 573–582.

- (67) Tesi, C.; Piroddi, N.; Colomo, F.; Poggesi, C. Relaxation Kinetics Following Sudden Ca^{2+} Reduction in Single Myofibrils from Skeletal Muscle. *Biophys. J.* **2002**, *83*, 2142–2151.
- (68) Campbell, K. S. Compliance Accelerates Relaxation in Muscle by Allowing Myosin Heads to Move Relative to Actin. *Biophys. J.* **2016**, *110*, 661–668.
- (69) Biesiadecki, B. J.; Kobayashi, T.; Walker, J. S.; John Solaro, R.; de Tombe, P. P. The Troponin C G159D Mutation Blunts Myofilament Desensitization Induced by Troponin I Ser23/24 Phosphorylation. *Circ. Res.* **2007**, *100*, 1486–1493.
- (70) Schmidtman, A.; Lindow, C.; Villard, S.; Heuser, A.; Mugge, A.; Gessner, R.; Granier, C.; Jaquet, K. Cardiac Troponin C-L29Q, Related to Hypertrophic Cardiomyopathy, Hinders the Transduction of the Protein Kinase a Dependent Phosphorylation Signal from Cardiac Troponin I to C. *FEBS J.* **2005**, *272*, 6087–6097.
- (71) Dong, W. J.; Xing, J.; Ouyang, Y. X.; An, J. L.; Cheung, H. C. Structural Kinetics of Cardiac Troponin C Mutants Linked to Familial Hypertrophic and Dilated Cardiomyopathy in Troponin Complexes. *J. Biol. Chem.* **2008**, *283*, 3424–3432.
- (72) Li, A. Y.; Stevens, C. M.; Liang, B.; Rayani, K.; Little, S.; Davis, J.; Tibbits, G. F. Familial Hypertrophic Cardiomyopathy Related Cardiac Troponin C L29Q Mutation Alters Length-Dependent Activation and Functional Effects of Phosphomimetic Troponin I. *PLoS One* **2013**, *8*, e79363.
- (73) Messer, A. E.; Bayliss, C. R.; El-Mezgueldi, M.; Redwood, C. S.; Ward, D. G.; Leung, M.-C.; Papadaki, M.; dos Remedios, C.; Marston, S. B. Mutations in Troponin T Associated with Hypertrophic Cardiomyopathy Increase Ca^{2+} -Sensitivity and Suppress the Modulation of Ca^{2+} -Sensitivity by Troponin I Phosphorylation. *Arch. Biochem. Biophys.* **2016**, DOI: [10.1016/j.abb.2016.03.027](https://doi.org/10.1016/j.abb.2016.03.027).
- (74) Deng, Y.; Schmidtman, A.; Kruse, S.; Filatov, V.; Heilmeyer, L. M. G.; Jaquet, K.; Thieleczek, R. Phosphorylation of Human Cardiac Troponin I G203S and K206Q Linked to Familial Hypertrophic Cardiomyopathy Affects Actomyosin Interaction in Different Ways. *J. Mol. Cell. Cardiol.* **2003**, *35*, 1365–1374.
- (75) Pinto, J. R.; Siegfried, J. D.; Parvatiyar, M. S.; Li, D. X.; Norton, N.; Jones, M. A.; Liang, J. S.; Potter, J. D.; Hershberger, R. E. Functional Characterization of Tnni1 Rare Variants Identified in Dilated Cardiomyopathy. *J. Biol. Chem.* **2011**, *286*, 34404–34412.
- (76) Finley, N.; Abbott, M. B.; Abusamhadneh, E.; Gaponenko, V.; Dong, W.-j.; Gasmi-Seabrook, G.; Howarth, J. W.; Rance, M.; Solaro, R. J.; Cheung, H. C.; et al. Nmr Analysis of Cardiac Troponin C-Troponin I Complexes: Effects of Phosphorylation. *FEBS Lett.* **1999**, *453*, 107–112.
- (77) Dohet, C.; AlHillawi, E.; Trayer, I. P.; Ruegg, J. C. Reconstitution of Skinned Cardiac Fibres with Human Recombinant Cardiac Troponin-I Mutants and Troponin-C. *FEBS Lett.* **1995**, *377*, 131–134.
- (78) Takimoto, E.; Soergel, D. G.; Janssen, P. M. L.; Stull, L. B.; Kass, D. A.; Murphy, A. M. Frequency- and Afterload-Dependent Cardiac Modulation in Vivo by Troponin I with Constitutively Active Protein Kinase a Phosphorylation Sites. *Circ. Res.* **2004**, *94*, 496–504.
- (79) Sakthivel, S.; Finley, N. L.; Rosevear, P. R.; Lorenz, J. N.; Gulick, J.; Kim, S.; VanBuren, P.; Martin, L. A.; Robbins, J. In Vivo and in Vitro Analysis of Cardiac Troponin I Phosphorylation. *J. Biol. Chem.* **2005**, *280*, 703–714.
- (80) Yamasaki, R.; Wu, Y.; McNabb, M.; Greaser, M.; Labeit, S.; Granzier, H. Protein Kinase a Phosphorylates Titin's Cardiac-Specific N2b Domain and Reduces Passive Tension in Rat Cardiac Myocytes. *Circ. Res.* **2002**, *90*, 1181–1188.
- (81) Colson, B. A.; Bekyarova, T.; Locher, M. R.; Fitzsimons, D. P.; Irving, T. C.; Moss, R. L. Protein Kinase a-Mediated Phosphorylation of Cmybp-C Increases Proximity of Myosin Heads to Actin in Resting Myocardium. *Circ. Res.* **2008**, *103*, 244–251.
- (82) Warren, C. M.; Kobayashi, T.; Solaro, R. J. Sites of Intra- and Intermolecular Cross-Linking of the N-Terminal Extension of Troponin I in Human Cardiac Whole Troponin Complex. *J. Biol. Chem.* **2009**, *284*, 14258–14266.
- (83) Dong, W. J.; Chandra, M.; Xing, J.; She, M. D.; Solaro, R. J.; Cheung, H. C. Phosphorylation-Induced Distance Change in a Cardiac Muscle Troponin I Mutant. *Biochemistry* **1997**, *36*, 6754–6761.
- (84) Heller, W. T.; Finley, N. L.; Dong, W. J.; Timmins, P.; Cheung, H. C.; Rosevear, P. R.; Trewella, J. Small-Angle Neutron Scattering with Contrast Variation Reveals Spatial Relationships between the Three Subunits in the Ternary Cardiac Troponin Complex and the Effects of Troponin I Phosphorylation. *Biochemistry* **2003**, *42*, 7790–7800.
- (85) Reiffert, S. U.; Jaquet, K.; Heilmeyer, L. M. G.; Herberg, F. W. Stepwise Subunit Interaction Changes by Mono- and Bisphosphorylation of Cardiac Troponin I. *Biochemistry* **1998**, *37*, 13516–13525.